Stable isotopes of soil provide insights into hominin paleoenvironments in the Khovaling Loess Plateau of Southern Tajikistan, Central Asia

Aljasil Chirakkal[1*], Ekaterina Kulakova[2], Jago Jonathan Birk[3], Anton Anoikin[4], Redzhep Kurbanov[5], Petr Sosin[6], Peixian Shu[7], David K. Wright[1]

[1]Department of Archaeology, Conservation and History, University of Oslo, Oslo, Norway

[2]Institute of Physics of the Earth RAS, Moscow, Russia

[3]Department of Geography, University of Göttingen, Göttingen, Germany

[4]Institute of Archaeology and Ethnography SB RAS, Novosibirsk, Russia

[5]Institute of Geography RAS, Moscow, Russia

[6]Institute of Water Problems, Hydropower and Ecology NAST, Dushanbe, Tajikistan

[7]Institute of Earth Environment, Chinese Academy of Sciences, Xi'an, China

***Corresponding Authors**

Aljasil Chirakkal

[1]Institute of Archaeology, Conservation and History, University of Oslo, Oslo, 0371, Norway.

jasilchirakkal@gmail.com

Abstract

Here, we present the first soil isotopic record in association with Paleolithic occupations in the Khovaling Loess Plateau of Southern Tajikistan, Central Asia. This region has been the focus of numerous archaeological projects since Soviet times as it contains evidence of some of the oldest (~0.9 Ma) hominin occupations in Central Asia and is one of the key regions connecting eastern Asia to centers of hominin evolution that lie to the west. Previous archaeological surveys discovered rich collections of lithic artifacts concentrated in pedocomplexes (PCs) 4, 5, and 6 formed in eolian deposits corresponding to Marine Isotope Stages (MIS) 11 (364–427 ka), MIS 13 (474–528 ka), and MIS 15 (563–621 ka), respectively, from many loess-paleosol locales, such as Karatau, Lakhuti, Obi-Mazar, and others. Here, we use the soil organic matter stable carbon ($\delta^{13}C$) and nitrogen ($\delta^{15}N$) together with soil total organic carbon (TOC) and total nitrogen (TN) contents at four distinct landscape aspects relative to archaeological materials: on-site, sparse on-site, near-site, and off-site based archaeological findings in Khovaling loess record. Our results reveal that on-site locations are characterized by elevated $\delta^{15}N$ values and depleted $\delta^{13}C$ values indicating intensive human occupation and reliance on C_3 vegetation, indicative of cooler and wetter climate conditions. These findings are corroborated by the high concentrations of lithic artifacts at these locations, suggesting repeated episodes of human activity and possible landscape management compared to other locales. In contrast, near-site and off-site locations exhibit lower $\delta^{15}N$ values and higher $\delta^{13}C$ values with fewer or no lithic artifacts indicating less intensive human use and a shift towards more grassier vegetation and more open land cover conditions. This study highlights the significant role of early humans in shaping their environments, contributing to a deeper understanding of subsistence strategies and environmental adaptations during the Middle Pleistocene. Our findings highlight the importance of integrating isotopic data with archaeological evidence to reconstruct past human impacts on the landscape.

Keywords

Early Paleolithic, Human-environment, Isotope ecology, Loessic geoarchaeology, Pleistocene, Soil organic contents

1. Introduction

Changes in past climate conditions that enabled the spread of grasslands in the ancestral homelands of hominins are interpreted as having been critical landscape-level circumstances associated with significant milestones in human evolution, such as bipedal anatomical adaptations, technological innovation, and diversification of human populations (Cerling et al., 2011; Lupien et al., 2020). Archaeological/paleoanthropological studies and theoretical models have been developed to quantify these climate-human evolutionary relationships showing that climatic shifts played a significant role in shaping hominin adaptations, migrations, and technological innovations (Grove, 2014; Kingston, 2007; Lupien et al., 2020; Potts and Faith, 2015 and references therein). Based on climate-human evolution models, Asia is subdivided into two main pan-archaeological regions: 'Westerlies Asia' (i.e. the arid central region of SW China and Central Asia) and 'Monsoonal Asia' (i.e. the eastern and southern regions). The behavior of humans, including long-term technological variability, occupation intensity, and livelihood activities during the mid-late Pleistocene, tends to bifurcate according to these macroregions (An et al., 2012; Caves et al., 2015; Chen et al., 2019; Dennell, 2013; Dodonov, 1991; Gao et al., 2017; Kirsten et al., 2023; Ranov, 1995; Ranov et al., 1995; Ranov and Davis, 1979; Schäfer et al., 1998). In turn, Central Asia is further divided into two regions that differ both climatically and in terms of the specifics of their archaeological industries. In the Caspian zone and the northern part of the region (Kyrgyzstan, Kazakhstan), assemblages are found that include hand-axes and are considered by researchers within the framework of the Acheulean tradition (Davis and Ranov, 1999; Finestone et al., 2022; Glantz, 2011). However, in the southern part of the region (Tajikistan), Early Paleolithic sites belong to another cultural tradition, which lacks bifaces but contains a significant number of pebble choppers and unifacial tools (Ranov, 1995; Ranov et al., 1995; Ranov and Davis, 1979; Schäfer et al., 1998).

The existing interpretations of hominin behavior from this region hypothesize that interglacial times were characterized by warm and wet periods with high precipitation, which resulted in intensified pedogenesis, resource-rich zones, and forest-grassland mosaics ripe for human exploitation across vast portions of Southern Tajikistan (Dodonov and Baiguzina, 1995; Mestdagh et al., 1999; Ranov, 1995; Yang et al., 2006). There are also several significant riparian zones with high-quality raw materials for knapping that are not ubiquitous in the loess-covered landscapes of the region. These conditions supported the manufacture of expedient Paleolithic technologies,

which is evidenced by the presence of several lithic-bearing archaeological sites within river valleys (Ranov and Davis, 1979; Schäfer et al., 1998). In contrast, glacial periods were characterized by greater aridity, cooler temperatures, and the spread of mosaic environments (Pakhomov, 2006; Parviz et al., 2020) which, apparently, had a less suitable environment for hominins based on the almost complete absence of lithic artifacts in the loess layers corresponding to glacial periods.

The Khovaling Loess Plateau (KLP) of Southern Tajikistan is a promising area to contribute to a broad understanding of Eurasian human evolution and migration through the reconstruction of vegetation regimes associated with Early Pleistocene *Homo* species occupations. From an ecological and climatological perspective, the KLP consists of loess-paleosol sequences with sufficient thickness for a thorough study of paleoecological changes that occurred during the accumulation of wind-blown loess deposits and also their mid-continental location reflects linkages with global climate events (Buylaert et al., 2024; Challier et al., 2024; Meshcheryakova et al., 2023). Furthermore, these eolian deposits are associated with the earliest archaeological evidence of human settlement in Central Asia, reflecting the general technological and subsistence strategies of early hominins (Ranov, 1995; Schäfer et al., 1998). Since the second half of the 20th century, more than a dozen Early and Middle Paleolithic sites associated with loess-soil formations have been discovered in Tajikistan (Lazarenko, 1992; Ranov, 1989; Ranov and Zhukov, 1979; Ranov and Davis, 1979). Vladim Ranov, who discovered and studied these sites, grouped their materials into a single phenomenon known as the "Loess Paleolithic" (Ranov, 1995; Schäfer et al., 1998). Almost all archaeological materials are found within paleosols, called pedocomplexes (PCs) that are numbered sequentially from the most recent (PC 0, Holocene). At present, eight loess Paleolithic sites in Tajikistan are known to contain extensive archaeological materials: Kuldara (PC 12-11), Obi-Mazar-VI (PC 6), Karatau (PC 6), Lakhuti-IV (PC 6-4), Lakhuti-I (PC 5), Obi-Mazar-IV (PC 4), Khonako-III (PC 4, 2, and 1), and Dusti (PC 1). Almost all of them are located in the middle reaches of the Obi-Mazar River (Anoikin et al., 2023).

It is believed that the settlement of the region began at the end of the Early Pleistocene. Based on the available materials, four main stages of the Loess Paleolithic industries in Tajikistan can be identified: (a) Early Paleolithic Kuldara stage (0.9 Ma), (b) Early Paleolithic Karatau stage (0.6–0.4 Ma), (c) Middle Paleolithic blade-based stage (0.2 Ma), and (d) Middle Paleolithic Levallois-

Mousterian stage (0.1 Ma). The present data suggest that the transition between industrial stages was primarily associated with population changes and major regional environmental events (Anoikin et al., 2023; Ranov, 1995; Schäfer et al., 1998).

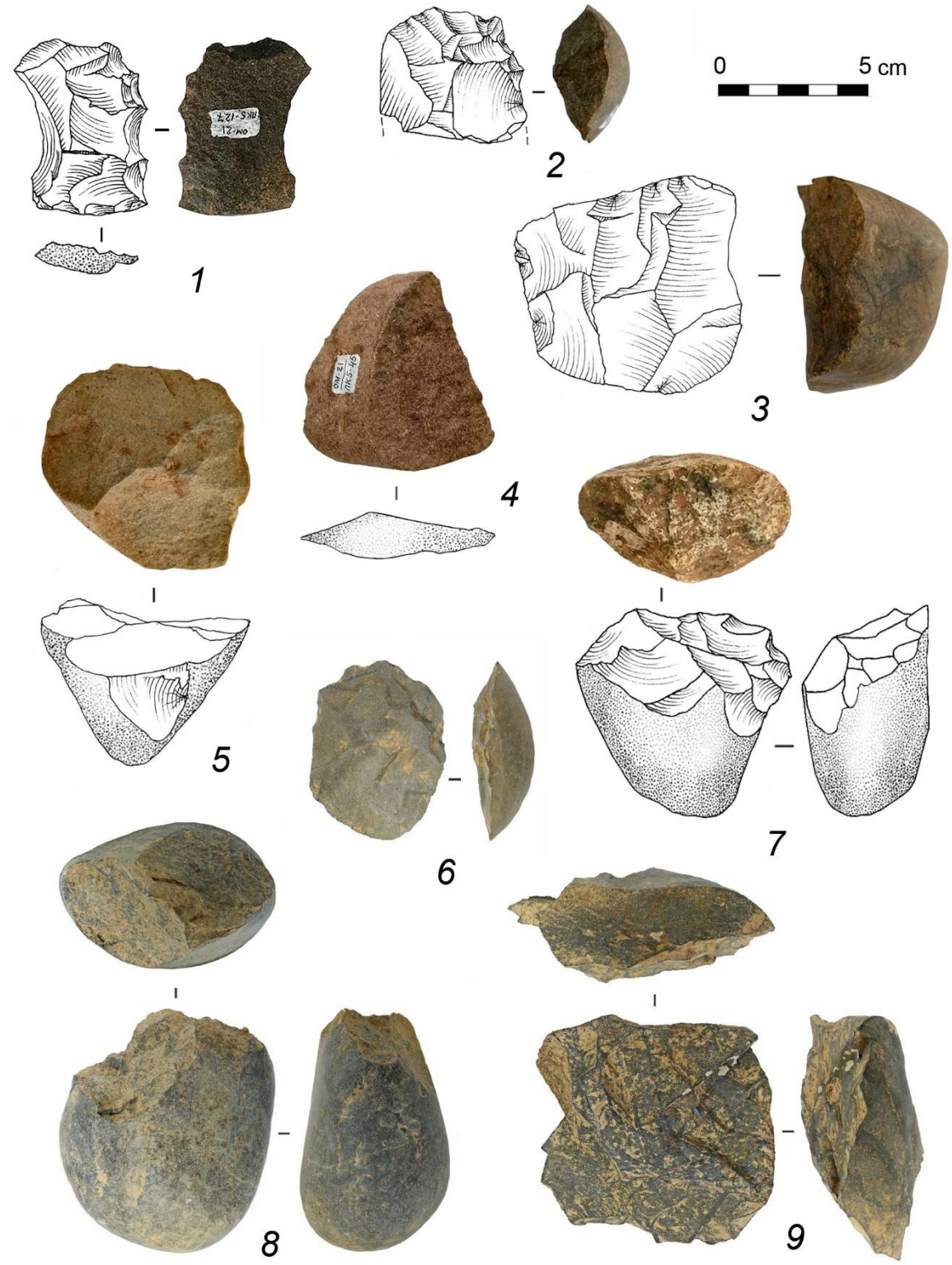

Fig. 1. Types of lithic artifacts excavated from the KLP locality (Lakhuti-IV site): 1, 6 - unifaces; 2 - denticulate tool; 3, 9 - radial cores; 4 - slice/”citrone”; 5 – slice core; 7, 8 - choppers.

The most representative Early Paleolithic technocomplex in Central Asia today is the Karatau culture, which existed in Tajikistan for approximately 200 ka (~0.6-0.4 Ma). The main archaeological assemblages from this period have been documented at the Obi-Mazar/Lakhuti sites, with over 4,000 lithic artifacts recorded. Despite the long existence of the Karatau culture, the stone industries at its sites belong to a single type and show very little variation. The primary knapping techniques employed were radial method, slice method, and parallel method, typically in their simplest, unidirectional form. Preparation of cores was either absent or minimal (one or two spalls). A small group of cores was found on large, massive flakes, with flake knapping on the ventral surface. Among the debitage, debris dominates (up to 70%). Formal blades are absent, but there are many blade-sized fragments present among the flakes. The toolkits include choppers, pebble side-scrapers, simple side-scrapers, denticulate and notched tools, as well as unifaces (fig. 1). There are also typical end-scrapers and a few points. The general analysis of the lithic assemblages associated with deposits from PC 6-4 reveals their industrial unity, defined by both preferred primary knapping techniques and composition of the toolkits. This technological stability, along with the association of assemblages with deposits of a single context (paleosols), suggests a potential link between the composition of the lithic industry and the environmental conditions in which the ancient hominins who produced these tools lived.

Our research complements paleoanthropological studies from Central Asia and Tajikistan by framing human-climate interactions within a long scope of adaptation and persistence over deep time cycles. The Pleistocene stratigraphy of the KLP comprises an alternation of loess (homogenous, wind-blown dust deposited generally under arid, cold conditions) and paleosols (ancient soils formed biogenically under warmer, moister conditions). Identifying links between Paleolithic industries, human behavior, and climate variability has been a long-standing academic endeavor and has a well-developed theoretical foundation in Asian paleoanthropology, archaeology, and geosciences (Chang, 1987; Dennell, 2008; Finestone et al., 2022; Ranov, 1995; Shen et al., 2017; Zeng et al., 2011). In such instances, the term "loessic geoarchaeology" has been proposed (Ranov, 1995). This approach relies on pedostratigraphy, stratigraphic associations, and classical sedimentology for qualitative analysis of human-environmental interactions.

This study augments established research by applying organic geochemical techniques and theoretical frameworks that have been extensively used in paleoanthropology and

paleoclimatology in Africa (Ambrose and Sikes, 1991; Cerling et al., 2011; Lupien et al., 2020; Thompson et al., 2021b). We measured total organic carbon (TOC), total nitrogen (TN), and stable carbon and nitrogen isotopes ($\delta^{13}C$, $\delta^{15}N$) in the KLP sequences to reconstruct vegetation structure and assess shifts between open and closed landscapes. These proxies provide insights into organic matter preservation, nitrogen cycling, and plant community composition in Early Paleolithic settings of southern Tajikistan. The isotope data are combined with physical characteristics of the loess-paleosol sequence units such as magnetic susceptibility to interpret paleoenvironmental conditions. By studying loess-paleosol sequences in the Khovaling region of Southern Tajikistan, we examine how similar or different from other loess regions like China and Europe are in terms of past vegetation and whether these changes in paleoenvironment are reflected in human activity and occupations.

2. Background

2.1 Khovaling Loess Plateau: Modern, Past Climatology and Lithostratigraphy

Modern climate data indicates that the study locales in Khovaling, Tajikistan experience a Mediterranean-type climate, characterized by dry summers and precipitation primarily occurring from early winter to spring. The modern mean annual temperature in Khovaling is 12.6°C, but significant seasonal temperature fluctuations occur, with variations exceeding 20°C between May and September due to its continental location (fig. 2a). While most of the precipitation, amounting to 663 mm annually, falls between October and June, with almost no rainfall from June to September (fig. 2b). Precipitation in the region is driven by Mediterranean cyclones and the Siberian Winter High, with moisture sourced either directly from the Mediterranean or North Atlantic Sea or recycled via the Black and Caspian Seas (Aizen et al., 2006; Dodonov and Baiguzina, 1995).

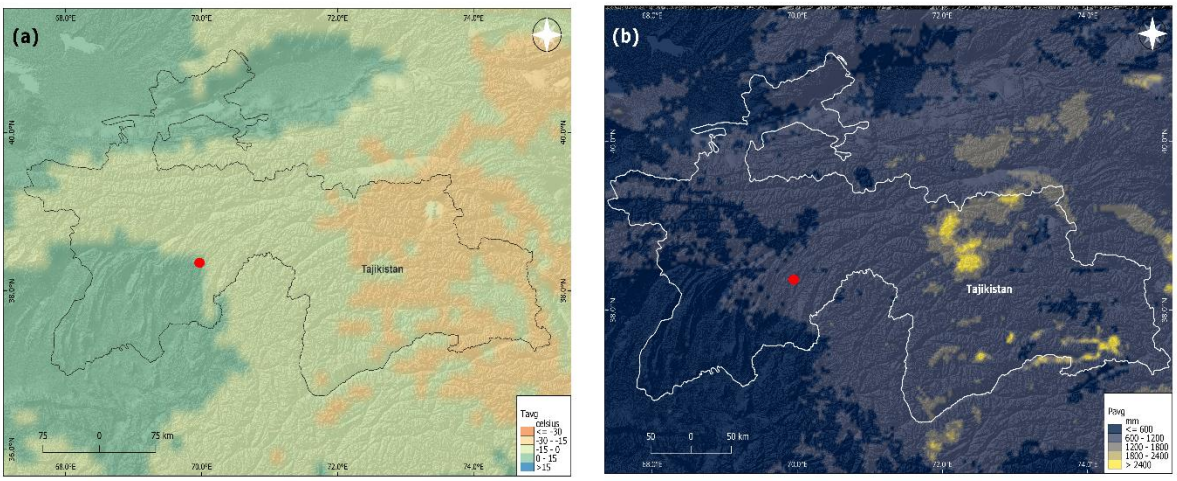

Fig. 2. (a) Average annual temperature (°C) and (b) average annual precipitation (mm) data of Khovaling region of Tajikistan (source: Temperature and Precipitation information (2003-2023), https://crudata.uea.ac.uk/cru/data/hrg/). The red dot denotes the location of the KLP.

The Pleistocene climate of Tajikistan was shaped by a combination of long-term aridification and the cyclic oscillation between glacial and interglacial periods, driven by global climatic shifts and regional weather systems. The uplift of the Tibetan Plateau and associated orogenesis in the Tien Shan, Pamir, and Hindu-Kush mountain ranges played a crucial role in restricting moisture penetration into Tajikistan from monsoonal systems (Li et al., 2019; Miao et al., 2012). This tectonic uplift intensified throughout the Pleistocene, further isolating the region from South Asian monsoonal influence, particularly after the Mid-Pleistocene Transition (MPT) between 1.2 and 0.8 Ma (Dodonov et al., 1999). The resulting aridification was accompanied by reduced monsoonal activity and the increasing dominance of continental high-pressure systems, such as the Siberian-Mongolian Anticyclone, which suppressed precipitation and enhanced eolian processes (Dodonov and Baiguzina, 1995; Shahgedanova, 2003). During glacial periods, intensified aridity, reduced vegetation cover, and stronger eolian activity contributed to extensive loess deposition, with continental high-pressure systems limiting the intrusion of westerlies (Ding et al., 2002). In contrast, interglacial periods have a greater influence from North Atlantic-Mediterranean westerlies, resulting in more humid conditions (Dodonov and Baiguzina, 1995). Due to limited moisture availability, glacial advances in Tajikistan were asynchronous with those in the Western Hemisphere (Abramowski et al., 2006). Additionally, the influence of the Asiatic Polar Front

during the Late Pleistocene in shaping eolian dynamics suggests that its role likely extended further back in time, alongside the interplay of westerlies and the Siberian-Mongolian Anticyclone (Machalett et al., 2008).

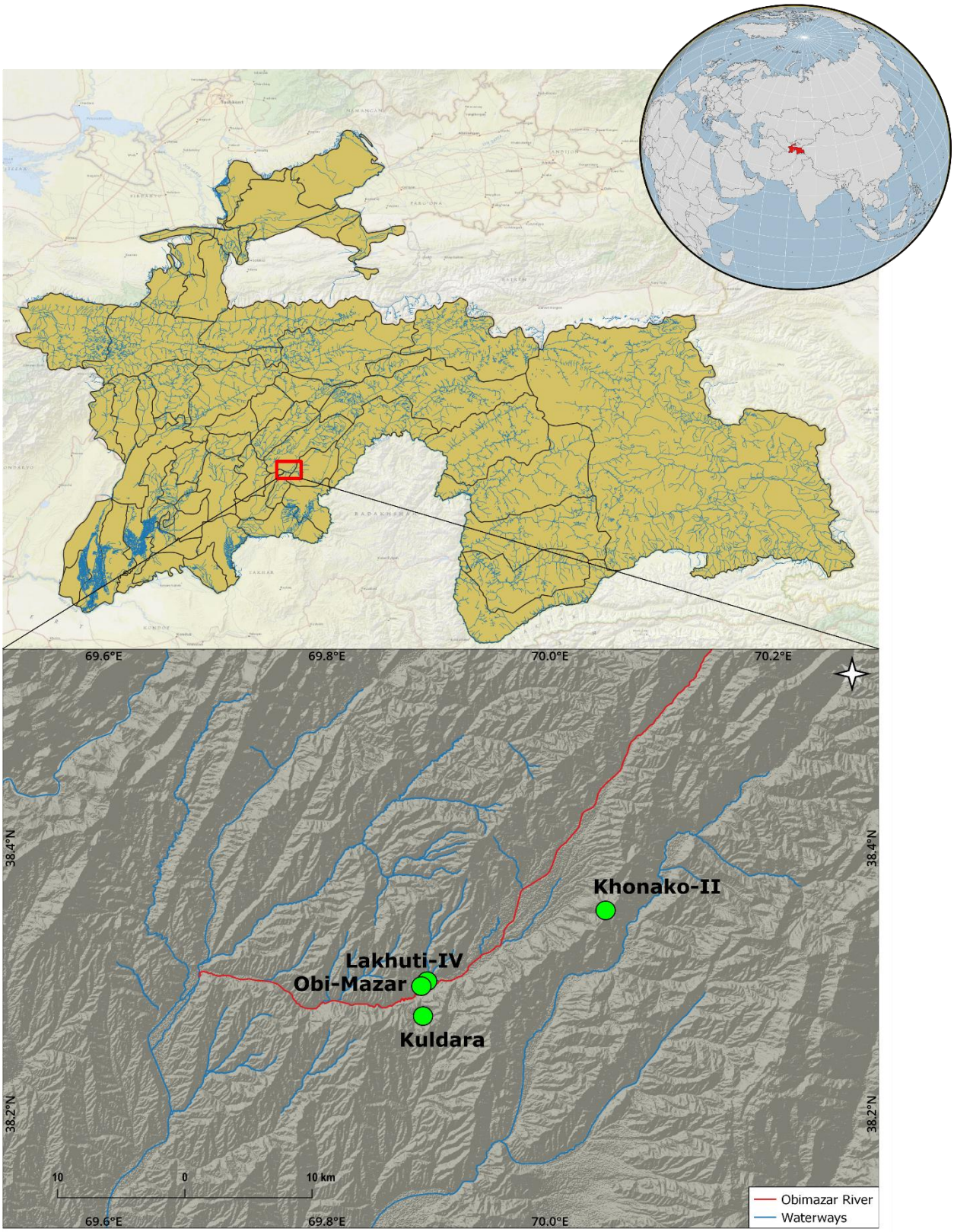
69.6°E
69.8°E
70.0°E
70.2°E
38.4°N
38.2°N
Khonako-II
Lakhuti-IV
Obi-Mazar
Kuldara
10
0
10 km
Obimazar River
Waterways

188

Fig. 3. Location of archaeological sites on the Khovaling Loess Plateau (KLP) in Southern Tajikistan.

Our study locales are defined by four loess-paleosol sequences located around the valley of the Obi-Mazar River in the Khovaling district of Southern Tajikistan (fig. 3). In this context, a "site" refers to a distinct location within the loess-paleosol sequences that contains evidence of past human presence, specifically through the discovery of lithic artifacts. In this context, archaeological sites are easily identified because the sedimentary matrix consists exclusively of silt- or clay-sized particles (Tokareva et al., 2025) and there are no proximal colluvial or alluvial sources of stones, meaning that large clasts are, by definition, manuports. Therefore, the distribution and concentration of these artifacts serve as indicators of human activity and occupation intensity during the time intervals recorded in the sequence. The first site is Lakhuti-IV (LK-IV), located in the north-east of the Obi-Mazar/Lakhuti outcrop, 50 m above the Obi-Mazar River (38.29° N, 69.89° E) (fig. 3 and 4a). This outcrop is formed by a unit of alluvial pebbles 20-40 m thick, overlain by a thick (up to 90 m) loess-paleosol sequence, including seven pedocomplexes, and extends about 1.5 km north-east along the river. The rich collection of lithic artifacts was obtained from pedocomplexes (PCs) 4, 5, and 6 in the Russian-Tajik geoarchaeological expedition in 2021-2023 (Anoikin et al., 2023).

The second site is Obi-Mazar (OBM), located in the middle of the Obi-Mazar/Lakhuti outcrop (38.28° N, 69.88° E) (fig. 3 and 4b), also includes seven pedocomplexes, which have a thickness of 90 m from the bottom of PC 7 to the Holocene soil. At the end of the 20th century, excavations at the OBM-IV and -VI sites uncovered a substantial collection of lithic artifacts (about 1,500 items). However, significant portions of these sites were later destroyed by a massive landslide. The modern Obi-Mazar section is more than 100 m inland from the original sites and represents their periphery. The third site is Kuldara (KUL), located ~2 km far from the Obi-Mazar/Lakhuti outcrop, includes up to 12 pedocomplexes and has a loess depth of 85 m (38.27° N, 69.88° E) (fig. 3 and 4c). It is worth noting that the site is located on a small tributary of the Obi-Mazar River, few kilometers from the main valley and primary sources of lithic raw materials. This may explain the relatively small collection of artifacts and the apparent low intensity of occupation in antiquity. A few stone tools were discovered from PCs 4, 5, 6, and 10 at Kuldara by the Russian-Tajik geoarchaeological expedition in 2021 (Kulakova et al., 2024), while this site is more known for

the oldest lithic artifacts findings (40 items) in the region in PCs 11-12 (Ranov, 1995). The fourth site is Khonako-II (KH-II), located on the Khonako outcrop which is ~15 km north-east of the group of other sites (38.35 ° N, 70.04° E) (fig. 3 and 4d). KH-II is 180 m thick and consists of up to 24 pedocomplexes (Dodonov, 1986). The KH-II section contains almost no archaeological material, with only a few artifacts found in PC 4. This section represents a far peripheral part of the Khonako-III site, located within the same exposure, where Middle Paleolithic artifacts were found in PC 1-2 (about 600 items), and Early Paleolithic artifacts in PC 4 (about 200 items). Additionally, a few artifacts were found in PC 6 (Ranov, 1995; Schäfer et al., 1998).

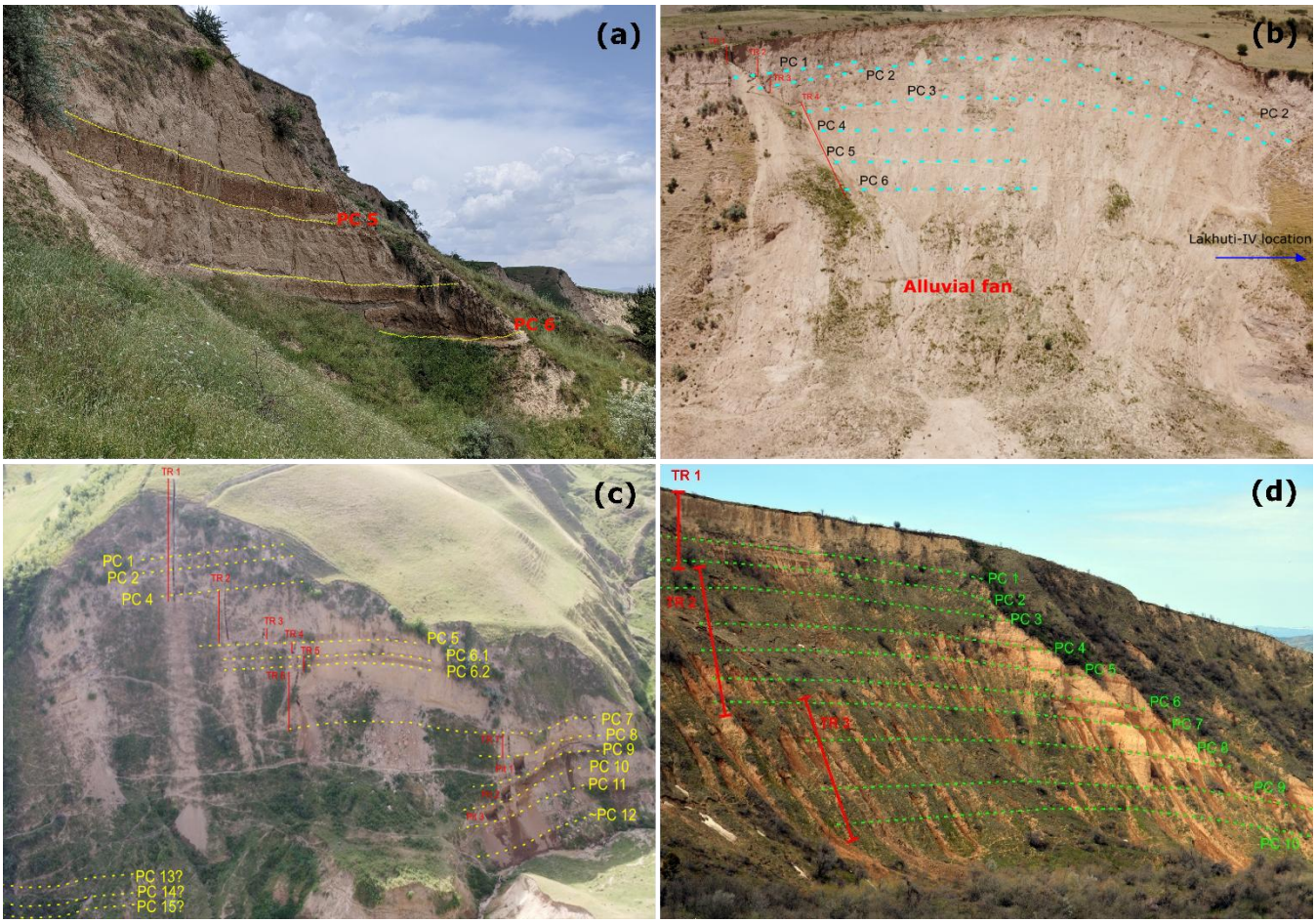

Fig. 4. Field photograph of stratigraphy and general view of the (a) LakhutI-IV (LK-IV), (b) Obi-Mazar (OBM), (c) Kuldara (KUL) and (d) Khonako-II (KH-II). PC: pedocomplex, L: Loess, TR: trench.

2.2 Age model and stratigraphic correlations

The climate cycles recorded in Tajik loess have been correlated to the Chinese loess and deep-sea oxygen records, which formed the initial basis of the age model of the Tajik loess-paleosol sequences (Ding et al., 2002; Forster and Heller, 1994; Shackleton et al., 1995). Since the 1990s, magnetic susceptibility and grain size variations of Tajik loess locales have been compared and correlated with the astronomically tuned oxygen isotope records from the deep sea sediments using paleomagnetic data as additional time anchor points (Ding et al., 2002; Dodonov et al., 2006; Dodonov and Baiguzina, 1995; Forster and Heller, 1994; Shackleton et al., 1995). According to these chronostratigraphic correlations, the first nine pedocomplexes in Southern Tajikistan are within the Brunhes chron, where PC 1 corresponds to Marine Isotope Stage (MIS) 5, each subsequent pedocomplex (PC 2–7) corresponds to the subsequent interglacial, and the weakly developed PC 8 formed during a warm substage of the glacial stage MIS 18. The first paleomagnetic data found the Brunhes-Matuyama boundary in the glacial loess between PC 9 and 10 (Penkov and Gamov, 1980), but recent detailed studies confidently place it at the base of PC 9 (Kulakova and Kurbanov, 2023), serving as a reliable time control point for the correlation of PC 9 with MIS 19. The current age model of Tajik loess was verified by recent geochronological research of the uppermost PCs using Optically Stimulated Luminescence (OSL) to confirm the formation of PC 1 and PC 2 during MIS 5 (71-130 thousand years ago [Kya]) and MIS 7 (191-243 Kya), respectively (Buylaert et al., 2024; Challier et al., 2024). In this way, based on this age model, PC 4 corresponds to MIS 11 (364 – 427 Kya), PC 5 to MIS 13 (474 – 528 Kya), and PC 6 to MIS 15 (563 – 621 Kya).

2.3 Stable isotope reconstruction in soils

Soil stable isotopes have been incorporated widely in studies to reconstruct ancient environments which can give insights into the past environmental conditions ($\delta^{13}C$ and $\delta^{15}N$) (Ambrose, 1991; Cerling, 1984; DeNiro, 1987; Kingston, 2007; Wynn, 2007; Zech et al., 2007). Within aerobic mineral soils, $\delta^{13}C$ and $\delta^{15}N$ tend to increase with depth while total organic carbon (TOC) and total nitrogen (TN) decrease as microorganisms that feed on organic matter preferentially metabolize and respirate lighter isotopes leaving heavier isotopes behind (Boström et al., 2007; Högberg, 1997; Karimi Nezhad et al., 2022; Novák et al., 1999). The enrichment of $\delta^{13}C$ and $\delta^{15}N$ relative to vegetal ground cover averages ~1‰ (Natelhoffer and Fry, 1988) to as high as 2.5‰ (Boström

et al., 2007) have been found in controlled tracer experiments of boreal forest soils (see also Ambrose and Sikes 1991).

Carbon isotopic values ($\delta^{13}C$) of soil organic matter (SOM) depend on factors including atmospheric CO_2 contribution and photosynthetic pathway (C_3 versus C_4). As a result of photosynthesis, CO_2, H_2O, and sunlight are converted into carbohydrates in plants. Non-succulent plants follow two primary photosynthetic pathways: C_3 and C_4. Most trees and many temperate grasses utilize the C_3 (Calvin cycle) pathway, in which atmospheric CO_2 is initially fixed into a three-carbon molecule via an enzyme called RuBisCO. This process is more efficient under cooler, low-light, and high-moisture conditions but is less effective in environments with low CO_2 concentrations due to increased photorespiration. While in contrast, some grasses and herbs in warm, high-light, and arid or seasonally dry environments have evolved the C_4 pathway (Hatch-Slack cycle), which first fixes CO_2 into a four-carbon compound using an enzyme PEP carboxylase. This adaptation minimizes photorespiration and allows for more efficient carbon assimilation under high temperatures and low atmospheric CO_2 conditions (Cerling et al., 1989; Farquhar et al., 1989; O'Leary, 1988). During carbon fixation, C_3 plants fractionate more strongly against ^{13}C than C_4 plants. Plants utilizing the C_3 photosynthetic pathway exhibit low $\delta^{13}C$ values, ranging from -34 to -22 ‰ vs. the Vienna Pee Dee Belemnite (VPDB) standard, with a mean of $\delta^{13}C$ = -27 ‰ (Boutton, 1991). In contrast, plants employing the C_4 pathway display $\delta^{13}C$ values between -16 and -9 ‰ vs. VPDB, with an average of $\delta^{13}C$ = -13 ‰.

Since the study region experiences a Mediterranean climate, characterized by winter-dominated precipitation and reduced solar radiation during the wet season, these conditions favor the development of C_3 dominated biomes, including both grasslands and forested environments (Still et al., 2003). In the modern era, tropical and subtropical savanna regions are dominated by C_4 grasses, while higher latitudes and Mediterranean climates such as those found in the KLP region are dominated by C_3 grasses (Golubtsov, 2020; Sage et al., 1999; Taft et al., 2011). Nevertheless, C_4 vegetation, mostly from the Chenopodiaceae family, is distributed widely as native plants across Central Asia, representing the furthest north occurrence of these plants in the world (Toderich et al., 2007). Moreover, MIS 13-15, often referred to as a "super interglacial," was a period of enhanced seasonality and increased winter moisture, which likely further contributed to

the expansion of C_3 plant ecosystems (Cheng et al., 2012; Kutzbach et al., 2014; Orland et al., 2019; H. Wang et al., 2024).

In addition to the C_3 vs. C_4 distinctions related to carbon isotope fractionation, the "canopy effect" (eg., Bonafini et al., 2013) is a significant factor influencing $\delta^{13}C$ variability as expressed in soils and sediments. This effect arises from multiple interacting mechanisms contributing to $\delta^{13}C$ depletion in forested environments. First, in closed-canopy settings, plants growing near the forest floor incorporate ^{13}C-depleted microbially respired CO_2, whereas higher-set trees primarily assimilate atmospheric CO_2, leading to a gradient in $\delta^{13}C$ values (van der Merwe and Medina, 1991). Second, the low light conditions within the canopy can result in increased stomatal conductance in plants when water availability is not limiting, thereby enhancing ^{13}C discrimination and further depleting $\delta^{13}C$ values in shaded leaves (Farquhar et al., 1989). Third, hydraulic pressure differences within tall trees influence water transport, with lower-set leaves having greater water availability and consequently exhibiting more negative $\delta^{13}C$ values, while upper canopy leaves experience higher $\delta^{13}C$ due to reduced stomatal conductance under greater water stress (Farquhar et al., 1989). These combined factors contribute to the overall reduction of $\delta^{13}C$ in soil organic matter beneath dense forest cover relative to more open settings (Habinger et al., 2022; Hofman-Kamińska et al., 2018; Ibañez et al., 2021). Thus, both the photosynthetic pathway and canopy structure are key drivers of isotopic variability in soils, with more negative values signaling a more closed canopy structure and less negative values indicating more open, grassy conditions (Bonafini et al., 2013; Buchmann et al., 1997; van der Merwe and Medina, 1991).

The occurrence of the heavier isotope of nitrogen (^{15}N) in the atmosphere occurs at a ratio of 1:273 compared to the more abundant ^{14}N isotope. Nitrogen continuously cycles between the atmosphere, soil, plants, and animals through biological and geochemical processes (Amundson et al., 2003). Atmospheric nitrogen (N_2) is fixed by microbes or taken up by plants directly and incorporated into organic matter and eventually returned to the soil through decomposition. Microbial processes such as nitrification, denitrification, and mineralization regulate nitrogen transformations, which influence $\delta^{15}N$ isotopic composition in soil (Högberg, 1997). In natural ecosystems, nitrogen cycling differs between forested environments and grasslands. Forested soils typically have lower $\delta^{15}N$ values due to a closed nitrogen cycle, where most nitrogen is retained within vegetation and soil organic matter, leading to minimal isotopic fractionation. In contrast,

grassland soils often exhibit higher $\delta^{15}N$ values due to a more open nitrogen cycle, where nitrogen is frequently lost through leaching, volatilization, and microbial denitrification, enriching the remaining soil in $\delta^{15}N$ (Högberg, 1997). Generally, higher soil organic matter tends to correspond with higher $\delta^{15}N$ due to humification (Kramer et al., 2003; Liao et al., 2018; Shan et al., 2019).

However, human-induced disturbances can alter nitrogen cycling and isotopic signatures. Some studies have shown that clearing of vegetation in forests can accelerate nitrogen loss, leading to further enrichment of ^{15}N in soils, however, after many years it tends to restore the pre-clearance level (Pardo et al., 2002; Sah et al., 2006). Moreover, landscape burning, foddering, and grazing of livestock tend to increase ^{15}N in soil (Szpak, 2014), while studies of anthropogenic soils from within pastoral encampments in Kenya have demonstrated long-term enrichment of ^{15}N even in abandoned areas (Marshall et al., 2018; Shahack-Gross, 2017). According to Commisso and Nelson (2006), anthropogenic soils, particularly those linked with intensive land use and past human activities, tend to exhibit higher values of ^{15}N than non-anthropogenic soils, although such assumptions are normally made within agricultural or urban contexts, not Paleolithic forager contexts. Additionally, in arid environments, enhanced evaporation and nitrogen volatilization can increase ^{15}N values, making them a useful proxy for reconstructing past aridity (Amundson et al., 2003).

3. Materials and methods

3.1 Field method and sample collection

During the 2021 and 2022 fieldwork seasons, four loess-paleosol sequences were targeted for pedostratigraphic analysis and sampling at the Lakhuti-IV (LK-IV), Obi-Mazar (OBM), Kuldara (KUL), and Khonako-II (KH-II) locales. The mapping and sampling strategies employed were identical for all four study locales and consisted of procedures outlined in Chirakkal et al. (2025a) following standard geoarchaeological techniques using the United States Department of Agriculture methods (Schoenberger et al., 2012). Following the convention of decades of geoarchaeological research in the area, we called the pedostratigraphic unit designation “L” for loess and “PC” for pedocomplex/paleosol and numbering begins from the top (youngest layers) and increases sequentially toward the bottom (oldest layers) of the sections throughout the study. The sampling of each study locale was performed by sampling trenches that were cut into exposed profiles. Each trench location was selected carefully to avoid areas with pedogenic cracking,

surface vegetation with rhizomes that have penetrated L or PC lenses, or other disturbances that were interpreted as having compromised the integrity of *in situ* sediment or soil structures. The trenches were cut back from the modern surface by >50 cm to avoid contamination by modern organic matter and surface runoff. The samples for stable isotopes were collected from PCs 4, 5, and 6 from four study locales. We separated our study locales into LK-IV (on-site), OBM (sparse on-site), KUL (near-site), and KH-II (off-site) contexts based on the recovery of artifacts (lithics, bone) by archaeological teams. However, the PC 5 layer of OBM is considered a "near-site" archaeological context due to no or little human activity. We collected samples from both loess and paleosol contexts across all four study locations. Notably, the samples taken from the loess horizons, including those at OBM and KUL are categorized as representing an off-site context similar to KH-II. This classification is based on the understanding that the loess deposits, irrespective of their proximity to archaeological sites, reflect the broader environmental and sedimentary conditions of the region. Therefore, we treated all loess samples in the same analytical framework as off-site samples for comparative analysis. Sediment samples of ~50 g for stable isotope analysis per sampling point were retrieved in high-density polyethylene Whirl-paks using a trowel or knife, avoiding contact with human hands. All sample bags were kept open for drying at room temperature for >24 hours before repacking. Sample bags were checked daily to ensure that humidity did not accumulate and were further dried in a laboratory convection oven at 40°C for >72 hours immediately upon arrival in Oslo, Norway.

3.2 Magnetic susceptibility

Field magnetic susceptibility measurements were performed for the KUL, OBM, and LK-IV locales using a portable PIMV kappameter (Geodevice, Russia) with a sensitivity of up to 10^{-7} SI units. The measurement was carried out continuously over the entire thickness of sampling sections at the locales, the average step was about 3.5 cm. L4 and the majority of L5 at the LK-IV locale were not exposed by excavations, therefore these intervals were not measured. Measurement of the field magnetic susceptibility for the KH-II locale was incomplete, so for this locale, we provide the data of mass-specific magnetic susceptibility obtained from bulk samples. These loose, unoriented samples were collected at a 2-cm interval every 10 cm for paleosols and 20 cm for loess layers and air-dried in a laboratory for further measurements. Mass normalized magnetic susceptibility was measured using a MFK1-FA kappabridge (AGICO, Czech Republic) at a

frequency of 976 Hz and a field intensity of 200 A/m. The comparison of the field magnetic susceptibility and mass-specific measurements for the same locales (for eg., KH-II and KUL) showed identical behavior.

3.3 Stable isotope analysis

All samples for the study of stable carbon ($\delta^{13}C$) and nitrogen ($\delta^{15}N$) isotopes were homogenized using a sterile agate mortar and pestle. The sediment samples destined for analysis of $\delta^{13}C$ were saturated in 1M HCl for >24 hours to remove carbonates and the step was repeated if bubbles were still present. When the reaction with acid was stopped, distilled water was poured, which was added 3 times to the tubes, agitated, and centrifuged to complete the removal of carbonates and acid. Then samples were kept in an oven at 40°C with caps open until they were thoroughly dried. The samples for $\delta^{15}N$ measurements were not acidified. The $\delta^{13}C$ samples were weighed on a microbalance to 50±1 mg and $\delta^{15}N$ samples were weighed on a microbalance to 25±1 mg, then they were packed into sterile Tin capsules, with weights recorded to ±0.01 mg. The samples were then taken to the CLimate Interpretation of Plant Tissue (CLIPT) laboratory in the Department of Biosciences at the University of Oslo. Due to the financial crisis, CLIPT Laboratory was shut down in 2023. Therefore, we moved laboratory analyses to the Facility for advanced isotopic research and monitoring of weather, climate, and biogeochemical cycling (FARLAB) at the University of Bergen. However, both laboratories followed identical protocols to keep consistent measurements.

The soil organic matter components TOC and TN were analyzed using a Flash 1110 Elemental Analyser (EA) with a no-blank autosampler connected to a Delta V Plus isotope ratio mass spectrometer. Firstly, samples were combusted with excess O_2 at 1020ºC, then catalyzed with chromium oxide and silvered cobaltous oxide. The N-oxide molecules were reduced with a reducing agent, copper at 650ºC. A CO_2 trap was used for the $\delta^{15}N$ analyses and a water trap for both elements inside the system. The sodium percholate was used to clean the elemental analyser between the sample runs of $\delta^{13}C$ and $\delta^{15}N$ to ensure zero contamination of the instrument from CO "cracking" during $\delta^{13}C$ analysis, which can result in a residual mass of 28 molecules (^{12}C + ^{16}O) that could mimic as $^{14}N_2$ while $\delta^{15}N$ analysis. One set of triplicates was analyzed for every 10 samples, which is determined randomly. The standards utilized were IAEA-N1 and IAEA-N2 for N isotopes and USGS-24, IAEA-600, and IAEA-CH-6 for C isotopes (https://analytical-reference-materials.iaea.org/). The precision of standards was <0.2 per mille (‰).

3.4 Statistical methods

We conducted Shapiro-Wilks tests to assess the normality of TOC and TN data across the study collection points. This test is particularly suited for small to moderate sample sizes and evaluates whether the data deviates significantly from a normal distribution. Moreover, we applied two-sample t-tests and one-way ANOVA tests to compare stable isotopic ($\delta^{13}C$ and $\delta^{15}N$) data based on "on-site", "sparse on-site", "near-site" and off-site" contexts and assess whether there is a statistically significant difference between them. All statistical tests were conducted using open-source PAST software (Hammer et al., 2001). The correlations and tests of datasets were considered significant at p-value ≤ 0.05.

4. Results

4.1 Magnetic susceptibility

Magnetic susceptibility values demonstrate higher values in paleosols than in loess units (fig. 5), which is associated with the formation of ultrafine ferrimagnetic minerals (e.g. magnetite) during pedogenesis (Dodonov et al., 2002; Jia et al., 2018). Loess horizons are quite uniform in their magnetic properties, their mean values of magnetic susceptibility vary in the range of $2.8 – 3.0 \times 10^{-4}$ SI units. In paleosols, the values are, on average, 2× – 3.5× higher. Petrocalcite horizons, which are illuvial horizons of secondary precipitation of carbonates from overlying soil horizons, are characterized by low values of magnetic susceptibility due to abundant amounts of $CaCO_3$.

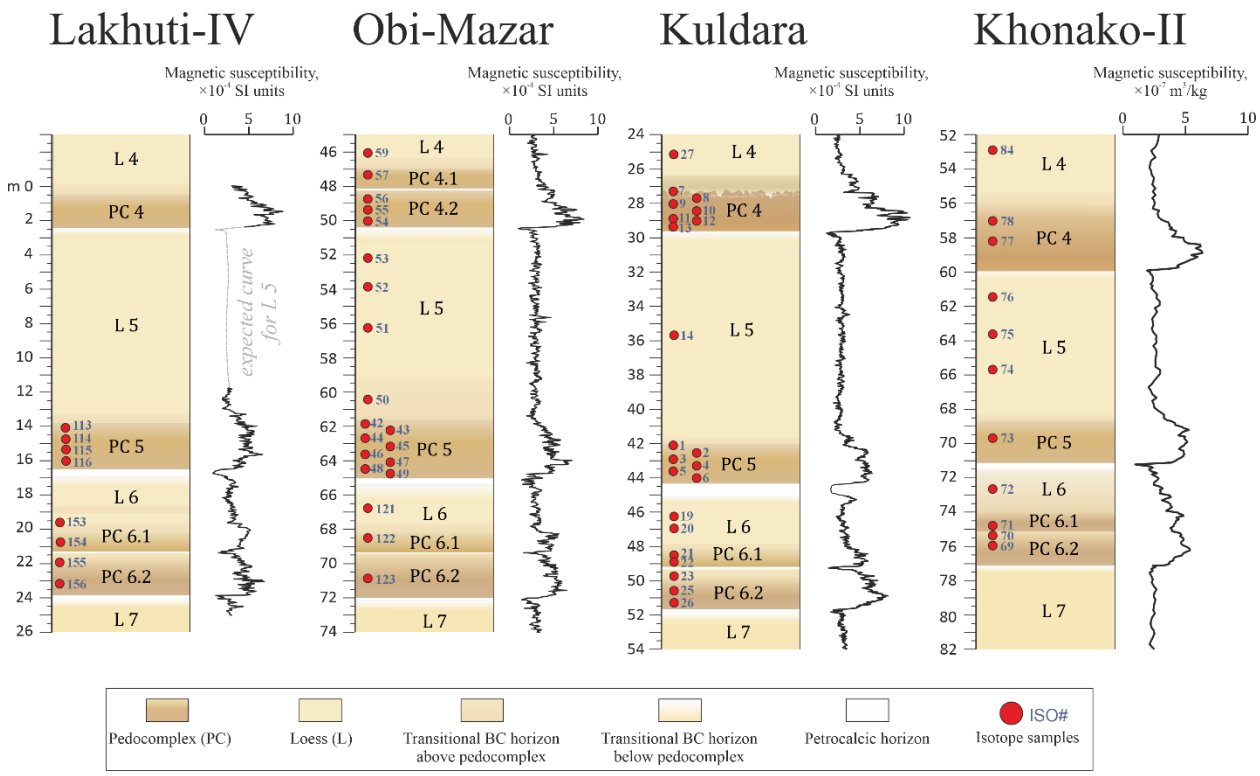

Fig. 5. Lithologic charts and magnetic susceptibility curves for PC 4-6 interval of Lakhuti-IV (LK-IV), Obi-Mazar (OBM), Kuldara (KUL), and Khonako-II (KH-II) locales.

Magnetic susceptibility can be used for stratigraphic correlation of the studied sections since each PC has its characteristic features. PC 4 is characterized by one sharp peak with maximum values up to 8.4 – 10.6 × 10^{-4} SI units. Sometimes two paleosols are distinguished in the structure of the PC (for example, OBM locale) by the presence of a thin petrocalcic (Bkk) horizon in the middle of the PC. However, the paleosol of the final stage of formation of the pedocomplex is weakly developed and does not have a separate peak according to magnetic susceptibility data. The magnetic susceptibility of PC 5 and PC 6 is slightly lower than that of PC 4 with maximum values of 7.0 – 8.1 × 10^{-4} SI units. PC 5 across the locales is characterized by one wide peak. PC 6 consists of two paleosols, sometimes intercalated with a thin (<50 cm) loess layer affected by soil formation processes. Both paleosols of PC 6 are well distinguished by two closely spaced peaks in magnetic susceptibility, in which the values are higher for the more developed paleosol PC 6.2.

4.2 Soil geochemistry

TOC and TN were also compared across the different study locales (LK-IV, OBM, KUL, and KH-II). A Shapiro-Wilks test of normality on TOC found that the variance is non-normally distributed

(W=0.904, p-value= <0.001) as was TN (W=0.871, p-value= <0.001). Boxplots of the data show that TOC and TN are significantly higher within LK-IV vs. OBM, KUL, and KH-II. Moreover, there is no statistical overlap at all in TOC from KH-II and the other locales, while TN from OBM, KUL, and KH-II show overlapping (fig. 6) with a decreasing mean value based on inferred distance from a known archaeological site location.

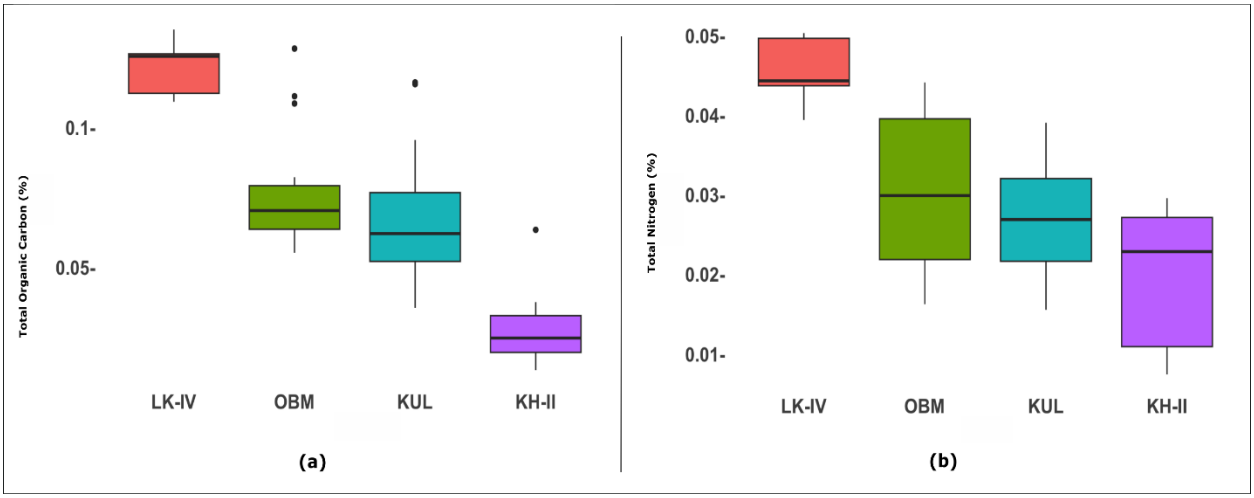

Fig. 6. (a) Total Organic Carbon (%) and (b) Total Nitrogen (%) of study sites sampled from KLP, Tajikistan.

To control for isotopic variability based on stratigraphical lithological layers (fig. 6), statistical tests were also performed to evaluate the effects of soil or sediment and relative depth. A one-way ANOVA test was conducted to compare the effect of various lithological layers on $\delta^{13}C$ values across six groups (L4, PC 4, L5, PC 5, L6, and PC 6). The analysis revealed a statistically significant difference in $\delta^{13}C$ values between the lithological layers (F=4.03, p=0.003, df=63). Similarly, the $\delta^{15}N$ content shows statistically significant differences between the lithological layers (F=9.29, p-value=0.001, df=63).

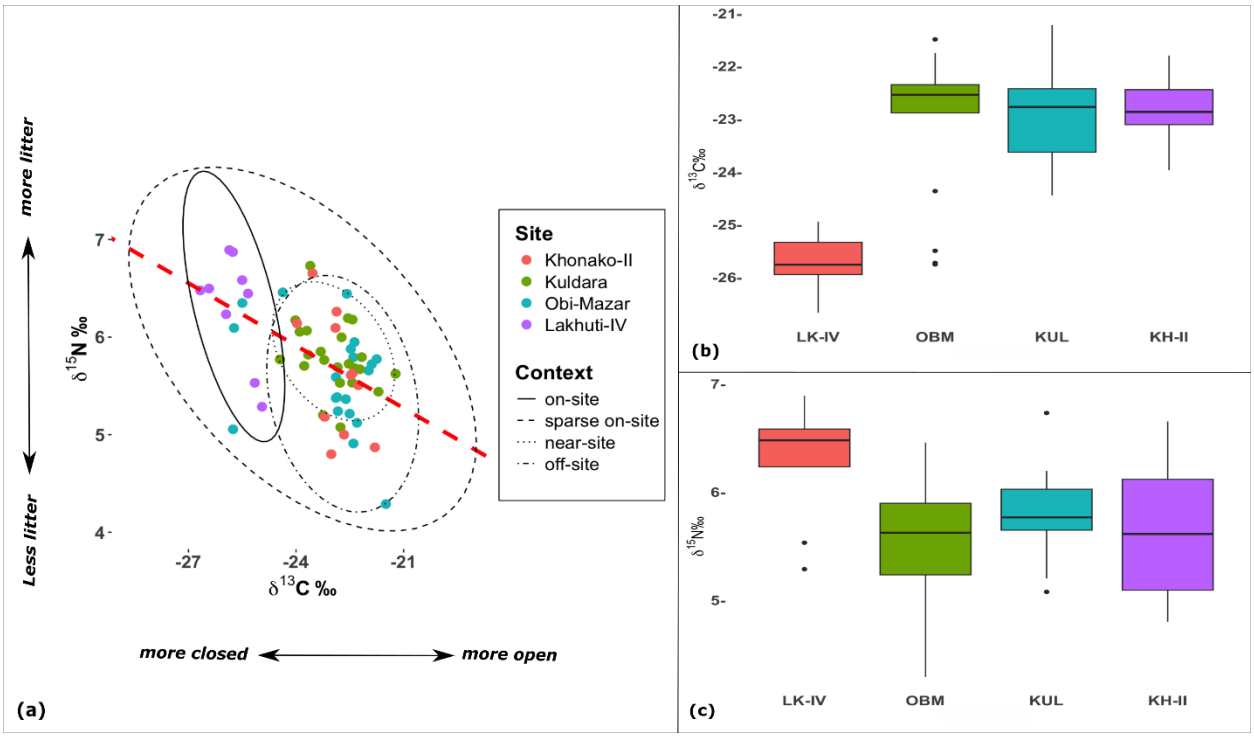

Fig. 7. (a) $\delta^{15}N$ (vs. AIR) plotted against $\delta^{13}C$ (vs. VPDB) values of soils based on-site (LK-IV), sparse on-site (OBM), near-site (KUL), and off-site (KH-II) contexts sampled from KLP, Tajikistan. The red dashed line shows a regression line with r^2 value of −0.213 showing inversely correlated enrichment of isotopic values. (b) 2-σ box plot of $\delta^{13}C$ by study site contexts. (c) 2-σ box plot of $\delta^{15}N$ by study site contexts.

Biplots of bulk soil stable isotopes conducted from the lithological categories on-site (LK-IV), sparse on-site (OBM), near-site (KUL), and off-site (KH-II as well as all L-horizons) show isotopic distributions with inversely correlated depleted $\delta^{13}C$ and elevated $\delta^{15}N$ levels located collectively at LK-IV relative to OBM, KUL and KH-II (fig 7; Table S1). However, OBM, KUL, and KH-II show overlapping values with one another, while LK-IV and KUL do not overlap (Fig 7b and c). The t-test was employed to determine whether a significant difference existed between the $\delta^{13}C$ and $\delta^{15}N$ data of the studied lithological layers. The t-test analysis of $\delta^{13}C$ revealed that LK-IV samples were statistically significantly lower than the OBM samples (t=6.08, p-value=0.0001, df=29). Additionally, LK-IV was also significantly less compared to KUL (t=9.88, p-value=0.0001, df=29) and KH-II (t=10.66, p-value=0.0001, df=19), although there was a statistically significant difference between LK-IV and these latter two locales. Moreover, a combination of archaeological soils context within 1 km (LK-IV + OBM) versus sparsely occupied

or non-archaeological soils (KUL + KH-II) also showed a statistically significant difference in which the former had significantly lower values than the latter (t=2.88, p-value=0.006, df=59). Finally, the combined archaeological soils context within a few km (LK-IV + OBM + KUL) versus non-archaeological/far off-site soils (KH-II) showed there was a statistically significant difference (t=1.50, p-value=0.01, df=59) between these collection contexts.

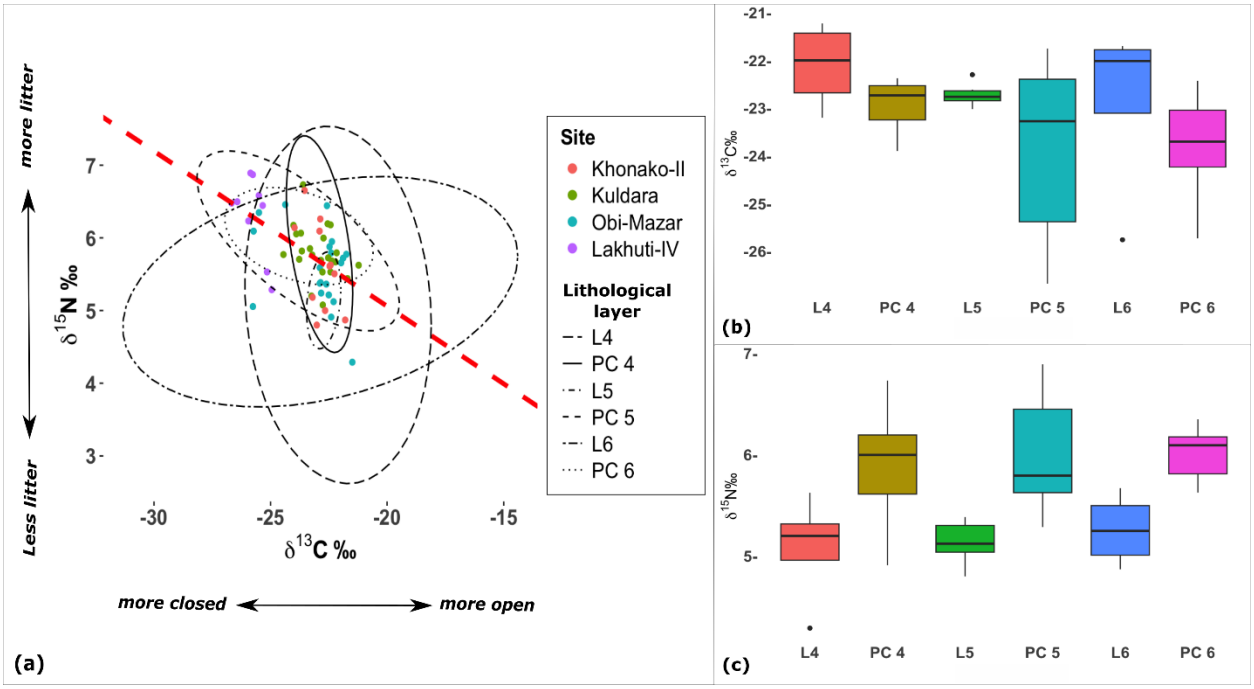

Fig. 8. (a) Biplot of $\delta^{13}C$ (vs. VPDB) and $\delta^{15}N$ (vs. AIR) values of lithological layer contexts sampled from study locales in KLP, Tajikistan. Regression line (dashed red): r^2 = -0.281. (b) 2-σ box plot of $\delta^{13}C$ by lithological layer contexts. (c) 2-σ box plot of $\delta^{15}N$ by lithological layer contexts.

Statistical analyses using t-tests of the $\delta^{15}N$ content further revealed statistically significant differences between LK-IV and OBM (t=3.33, p-value=0.003, df=29), with LK-IV being more isotopically elevated than OBM. Similarly, statistically significant differences were observed between LK-IV and KUL (t=3.71, p-value=0.014, df=29) and between LK-IV and KH-II (t=2.39, p-value=0.029, df=19), with LK-IV showing statistically higher values compared to both KUL and KH-II samples. However, the combined archaeological soils context within 1 km (LK-IV + OBM) versus sparsely occupied or non-archaeological soils (KUL + KH-II) showed no statistically significant differences (t=0.53, p-value=0.603, df=59). The combined anthropic soils context

within a few km (LK-IV + OBM + KUL) versus non-anthropic/far off-site soils (KH-II) also showed no statistically significant differences (t=0.65, p-value=0.514, df=59).

The plot of $\delta^{13}C$ (fig. 9) using stratigraphic inference with MIS ages shows that $\delta^{13}C$ values of the samples reveal significant shifts in organic source input across the MIS stages. During MIS 15, the $\delta^{13}C$ values were generally lower, particularly in on-site samples, suggesting a dominance of C_3 vegetation contributing to the formation of subsoils. During MIS 13 and MIS 11, the $\delta^{13}C$ values increase, reflecting a transition towards more C_4 / open vegetation contribution to SOM (fig. 9). Notably, on-site and sparse on-site samples consistently showed more depleted $\delta^{13}C$ values compared to near-site and off-site samples.

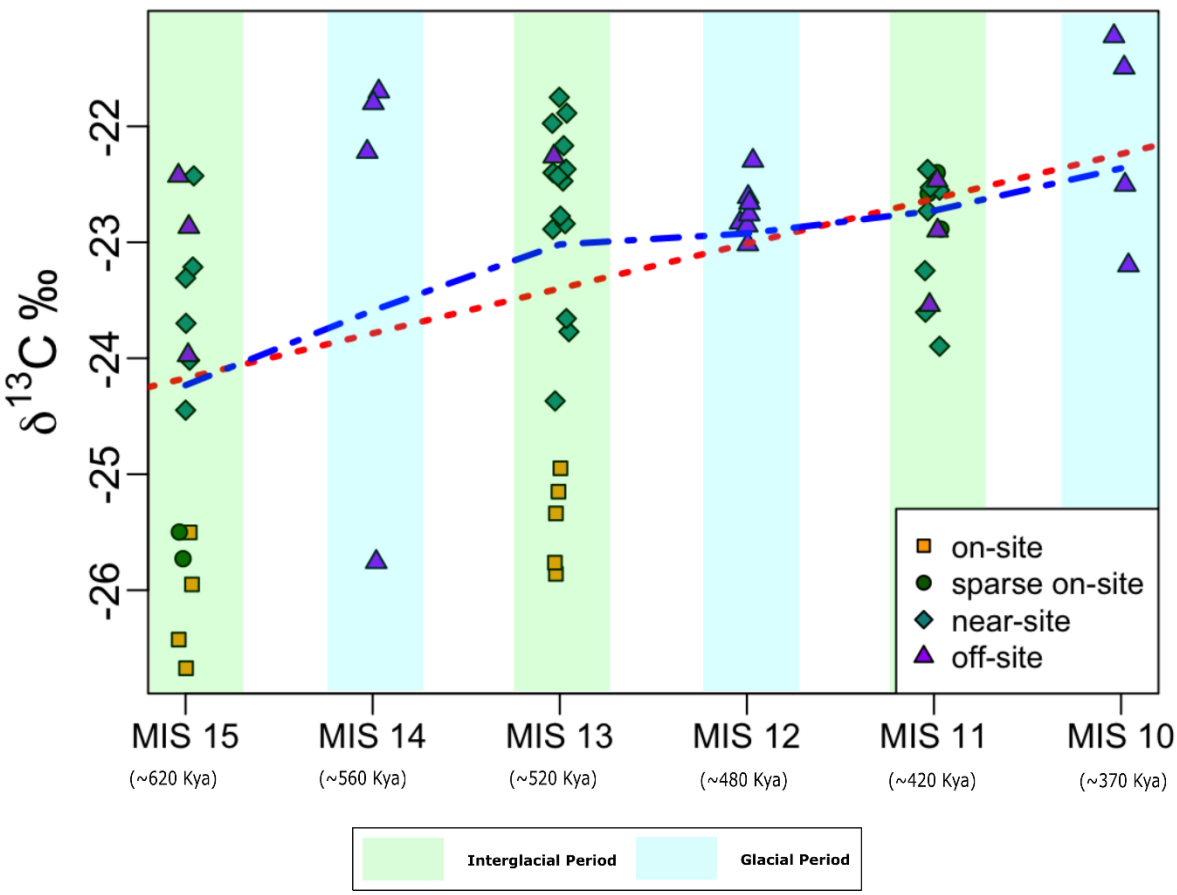

Fig. 9. Time-transgressive loess plot of $\delta^{13}C$ (vs. VPDB) of sediment samples from four study locales in the Khovaling Loess Plateau, Tajikistan. The red dotted line shows a regression line (r^2 value) of the plot of $\delta^{13}C$ (+0.45). The blue line shows the trend in $\delta^{13}C$ values from on-site to off-

site samples across Marine Isotope Stages (MIS), highlighting potential environmental and vegetation changes over time.

5. Discussion

This study primarily aimed to examine environmental changes in relation to hominin occupation of past landscapes in Central Asia during MIS 15-11 through the analysis of isotopic signatures ($\delta^{13}C$ and $\delta^{15}N$) and organic matter content (TOC and TN) across four distinct archaeological settings on the Khovaling Loess Plateau in Tajikistan, Central Asia: on-site (LK-IV), sparse on-site (OBM), near-site (KUL), and off-site (KH-II). These locations were selected based on their archaeological relevance and the varying degrees of human activity inferred from archaeological excavations undertaken since the 1970s (Anoikin et al., 2023; Ranov, 2000, 1995, 1989; Ranov et al., 1995; Ranov and Davis, 1979; Schäfer et al., 1998). Our analysis has revealed significant variations in $\delta^{13}C$ and $\delta^{15}N$ values across these locales, which provide insights into the types of vegetation present and the environmental conditions during the periods of occupation. Specifically, we observed statistically significantly depleted $\delta^{13}C$ (fig. 8b) and elevated $\delta^{15}N$ (fig. 8c) values at on-site locations reflecting a preponderance of C_3/closed vegetation, higher soil organic matter/ humification rates, and/or aridity.

The vegetation patterns in Central Asia are intricately tied to seasonal precipitation dynamics (Shen et al., 2018; Zhao et al., 2022). In Central Asia, C_4 vegetation grows best in warmer and drier climatic conditions and thrives with increased summer precipitation, whereas the C_3 vegetation is more commonly associated with cooler climates and winter/spring precipitation (Yang and Ding, 2006; Zhao et al., 2022). This seasonal difference in precipitation plays a key role in shaping the ecological landscape in this part of the world, as highlighted in studies on paleoclimate and vegetation dynamics (Häggi et al., 2019; Wang et al., 2024; Yang and Ding, 2006). The variability of seasonal moisture availability, thus, exerts a significant influence on the spread of C_3 and C_4 vegetation across Central Asia. Our interpretations of $\delta^{13}C$ values are further corroborated by biomarker analysis conducted on corresponding samples, where the presence of long-chain *n*-alkanes (C_{27}, C_{29}, C_{31}, and C_{33}) from plant waxes suggests a predominance of wood-dominated vegetation at the Lakhuti/Obi-Mazar locales during MIS 15-11 (Chirakkal et al., 2025b). These leaf wax biomarkers, which are highly resistant to degradation, provide a direct link

to the surrounding vegetation (Jha et al., 2024; Patalano et al., 2021), affirming the molecular fingerprints of a C_3-dominated landscape in this region.

While C_4 vegetation is relatively scarce in the study region due to the predominance of a Mediterranean climate with winter-dominated precipitation in relatively low-sunlight conditions, the observed $\delta^{13}C$ variability must also be considered in the context of vegetation structure rather than solely in terms of C_3 vs. C_4 plant distributions. Another prominent driver of $\delta^{13}C$ variability in this region is likely to be the "canopy effect," where dense vegetation can result in more depleted $\delta^{13}C$ values due to reduced photosynthetic discrimination in closed forest environments (Habinger et al., 2022; Hofman-Kamińska et al., 2018; Ibañez et al., 2021; van der Merwe and Medina, 1991). This effect is prevalent in forested or densely vegetated areas and likely contributed to the depleted $\delta^{13}C$ isotopic signatures we measured at LK-IV (Fig. 7b). Therefore, variations in $\delta^{13}C$ values between the study locales may reflect differences in canopy density, environmental conditions, or anthropogenic activities affecting local vegetation. This phenomenon has been documented in various forested and Mediterranean settings, where reduced light availability and increased soil carbon turnover under dense vegetation contribute to lower $\delta^{13}C$ values due to the recycling of depleted carbon pools (Aponte et al., 2010; Crowley et al., 2013; Roberts et al., 2017). Thus, the $\delta^{13}C$ signals observed in our record likely reflect not only shifts in plant functional types but also canopy density and associated biogeochemical processes.

A final source of potential variability related to the range of $\delta^{13}C$ values observed in our dataset is that it falls within the expected range for microbially degraded sedimentary organic carbon, as described by Wynn et al. (2005). Based on the negative correlations of $\delta^{13}C$ with TOC (R^2_{total} = 0.56; n = 63) and C/N (R^2_{total} = 0.57; n = 63) in cross-plot analyses (Fig. 9a and b, Table S1), at least some of the variations in $\delta^{13}C$ in the KLP are controlled by SOM degradation. Similarly, a positive correlation between TOC and C/N (R^2_{total} = 0.52, n = 63) (Fig. 9c, Table S1), likely reflects the influence of SOM degradation, where lower TOC content coincides with reduced C/N ratios due to the preferential loss of organic carbon. These interpretations were in agreement with findings by Zech et al. (2007) from the loess-paleosol sequence in the Tumara Valley of Northeast Siberia.

However, our recent findings (Chirakkal et al., 2025a) indicate an inverse relationship between short- and mid-chained alkanes (*n*-alkanes) and pyrogenic polycyclic aromatic hydrocarbons

(PAHs), suggesting that fire also significantly influenced the degradation of organic molecules. Thus, the combined effects of microbial degradation and fire may have contributed, at least in part, to the observed isotopic shifts. The $\delta^{13}C$ values align with the predictions of the Rayleigh distillation equation (Wynn et al., 2005), which provides a plausible explanation for progressive sedimentary organic carbon degradation and may indicate higher rates of pedogenesis in the study area. This suggests that the transformation of organic matter in these sediments was influenced by both biological and thermal processes, highlighting complex post-depositional alterations in the loess-paleosol sequences.

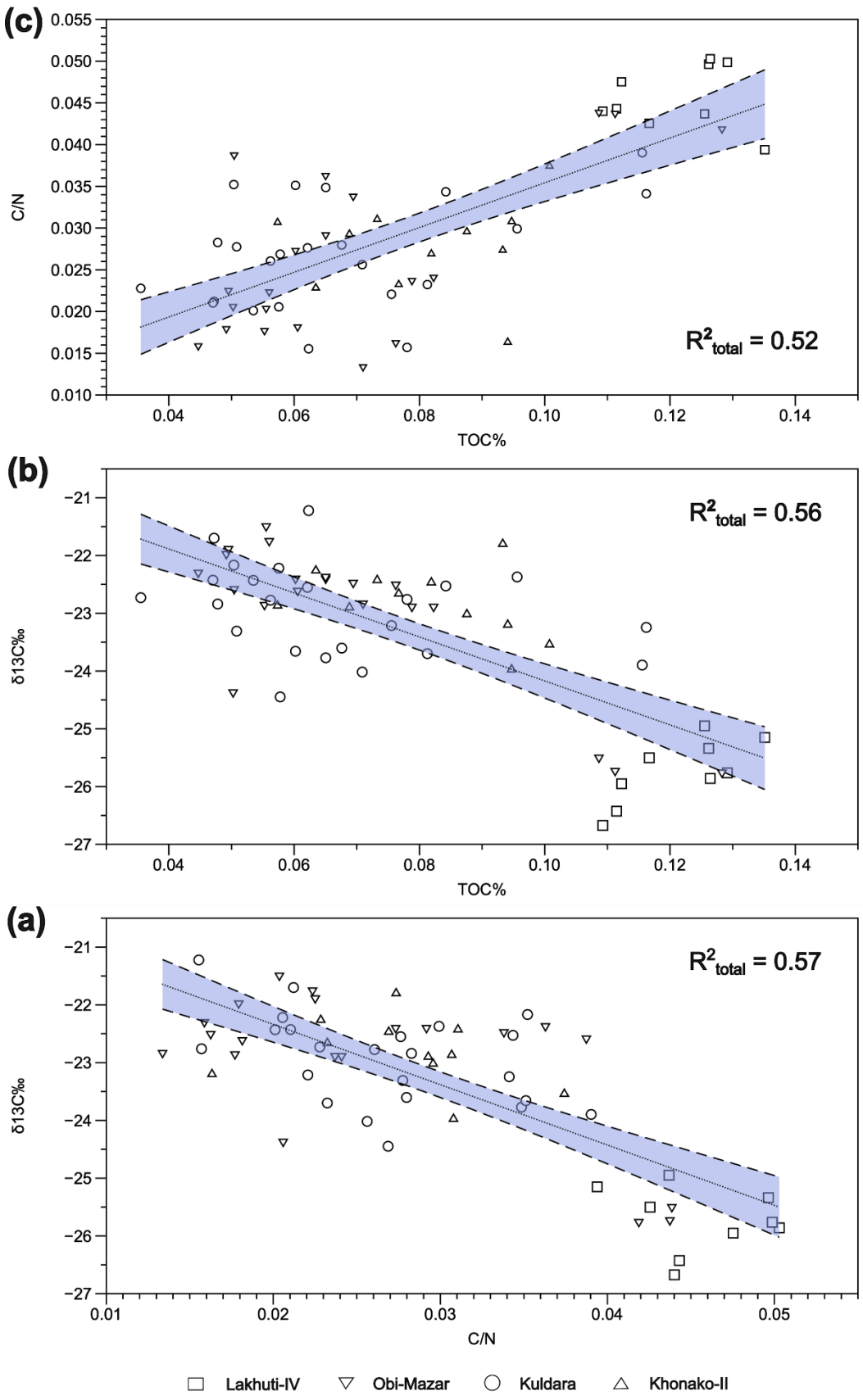
(c)
C/N
TOC%
R^2_{total} = 0.52
(b)
δ13C‰
TOC%
R^2_{total} = 0.56
(a)
δ13C‰
C/N
R^2_{total} = 0.57
Lakhuti-IV
Obi-Mazar
Kuldara
Khonako-II

576

Fig. 9. Correlation between $\delta^{13}C$, TOC, and C/N (n = 63): (a) $\delta^{13}C$ vs. C/N (R^2_{total} = 0.57), (b) $\delta^{13}C$ vs. TOC (R^2_{total} = 0.56) and (c) C/N vs. TOC (R^2_{total} = 0.52).

With these factors considered, our observed shifts in $\delta^{13}C$ values across the MIS stages (fig. 10) align with known climatic changes and isotope ecology during these periods in Tajikistan (Yang and Ding, 2006). The lower $\delta^{13}C$ values during MIS 15, correlated with speleothem $\delta^{18}O$ records (fig. 10d), suggest a landscape dominated by forests or woodlands and consistently enhanced winter and spring precipitation. This aligns with higher summer insolation and reduced global ice volume (fig. 10a and b) that characterize the early part of the "super interglacial" interval (Hao et al., 2015). However, the progressive enrichment in $\delta^{13}C$ values from MIS 13 to MIS 11 suggests an expansion of C_4 grasses or grassy C_3 landscapes, likely driven by an increase in summer rainfall, as indicated by elevated ^{10}Be precipitation proxies (fig. 10e). This phase of climate oscillation is consistent with benthic $\delta^{18}O$, reflecting large-scale glacial-interglacial variability (fig. 10b) that may have influenced vegetation shifts across Central Asia (Yang and Ding, 2006).

The broader transition towards open grassland ecosystems in the study region since 0.8 Ma is further supported by magnetic susceptibility data, where there is an observed trend of increasing magnetic susceptibility for loess-paleosol sections of Tajikistan starting from PC 4 (fig. 4) (Ding et al., 2002; Dodonov et al., 2006; Kulakova and Kurbanov, 2023; Mestdagh et al., 1999). The enhanced magnetic properties are connected to a higher concentration of ultrafine ferrimagnetic grains (e.g. magnetite and/or maghemite) in the superparamagnetic state, which also increases the frequency dependence of magnetic susceptibility (Jia et al., 2018; Kulakova and Kurbanov, 2023). Moreover, the preservation of ultrafine ferrimagnetics is typically associated with drier climates, which protects these particles from being washed out and transformed into hematite (Ahmed and Maher, 2018; Jordanova et al., 1997; Maher, 1998). The onset of the environmental transition that we observe from our isotopic data and corroborated by multiple paleoenvironmental proxies (fig. 10) may have made the region less attractive for hominin occupation of the region during the following interglacial (MIS 9), for which only a few lithic artifacts are known (Ranov, 2000).

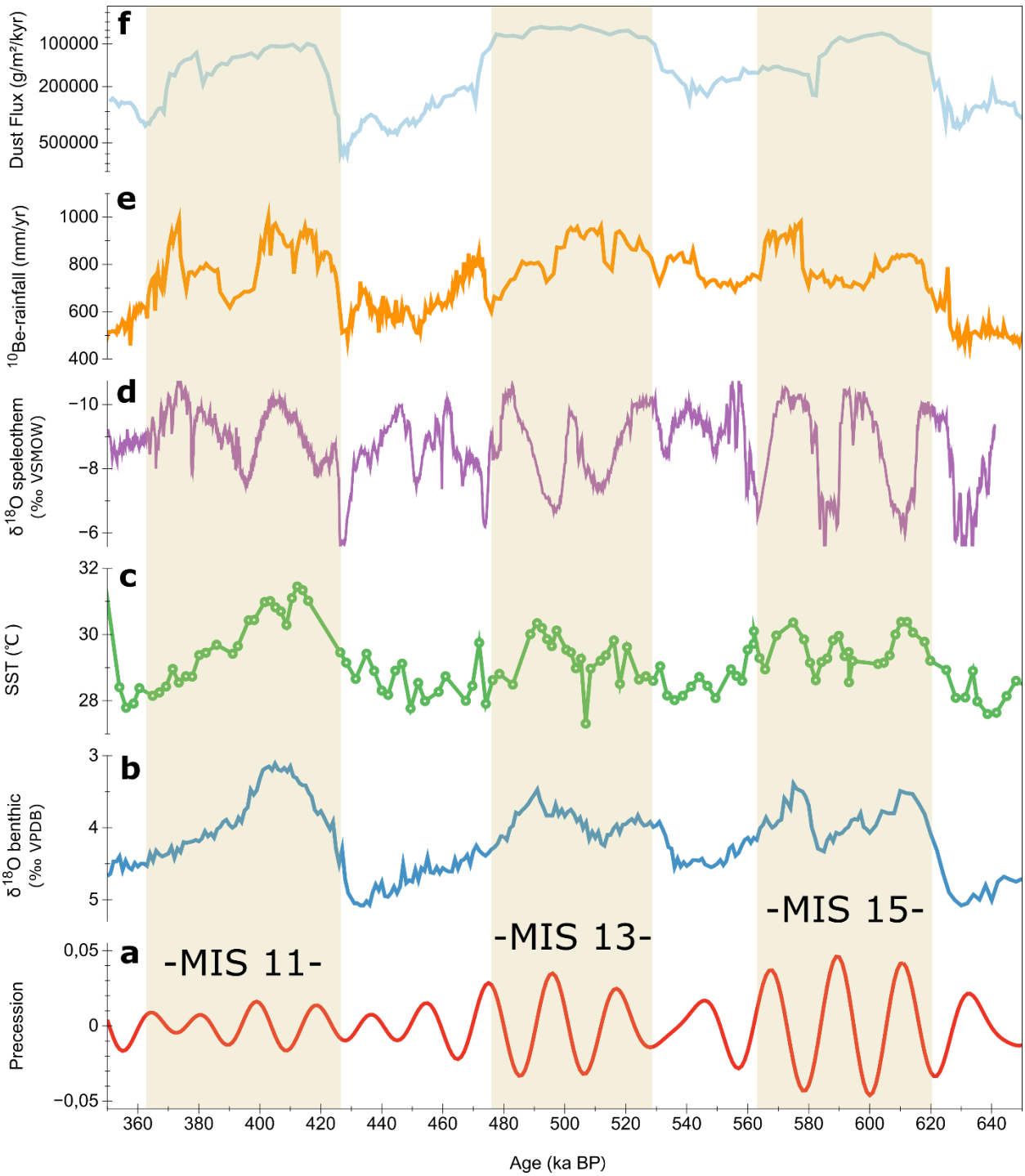

Fig. 10. An integrated multi-proxy reconstruction of climate variability during Marine Isotope Stages (MIS) (364–427 ka), MIS 13 (474–528 ka), and MIS 15 (563–621 ka) (highlighted in brown) **(a)** Orbital precession variability (Berger and Loutre, 1991), **(b)** $\delta^{18}O$ benthic stack as a global ice volume (Lisiecki and Raymo, 2005), **(c)** sea surface temperature variations (Clemens et

al., 2021), **(d)** $\delta^{18}O$ speleothem record (Cheng et al., 2016)**, (e)** ^{10}Be-derived precipitation estimates (Zhou et al., 2023), **(f)** eolian dust flux (Guo et al., 2009).

Elevated $\delta^{15}N$ values at the LK-IV location potentially indicate enhanced nitrogen recycling due to human activity or natural factors such as increased soil erosion, increased organic matter decomposition, and intensified fire regimes associated with past hominin disturbance, as well as aridification-driven changes in nitrogen dynamics (fig. 8c) (Hedges and Reynard, 2007; Szpak, 2014). The presence of can also contribute to $\delta^{15}N$ enrichment by promoting nitrogen volatilization and altering soil nitrogen dynamics (e.g., see Wang et al., 2021). The lower $\delta^{15}N$ values at the OBM, KUL, and KH-II locations than LK-IV may indicate reduced fire occurrence and more natural vegetation or soil processes (Mariotti, 1983). While soil $\delta^{15}N$ has been positively correlated to archaeological sites with evidence for agriculture, biochar amendment and paddocking (Larjavaara et al., 2017; Lauer et al., 2014; Szpak, 2014), to our knowledge, no study has heretofore examined relationships between elevated on-site $\delta^{15}N$ values from forager contexts and site activities. Nevertheless, differences observed in $\delta^{15}N$ values between the locales underscore the potential for spatial variability in human activity and its impact on the landscape. For example, fire events can lead to enhanced nitrogen retention in soils, particularly in areas of frequent burning, which would further influence isotopic signatures (Grogan et al., 2000; Huber et al., 2013; Rivas et al., 2012; Wang et al., 2021). The elevated $\delta^{15}N$ values observed at the LK-IV are consistent with biomarker evidence of frequent fire events, also indicated by elevated levels of pyrogenic PAHs in the sediments (Chirakkal et al., 2025b), which may have been anthropogenic in origin given their low occurrences in off-site contexts dating to the same time periods. In addition to this, comparative differences in TOC and TN measurements further underscore the distinct environmental settings and potential human influence on these locales (fig. 6).

The TOC and TN data provide valuable insights into the preservation and decomposition of organic matter across the different study locales. At the on-site and sparse on-site locations, higher TOC values suggest the presence of well-preserved organic matter. This could be attributed to human activities that actively promoted preservation vis-à-vis increased organic matter input, such as through the accumulation of habitation waste (Bianchi et al., 2024; Karkanas, 2010). Moreover, elevated TOC levels are indicative of environments where organic matter was either rapidly buried or consistently replenished, reducing the rate of decomposition and preservation of the carbon

content over time. The elevated pyrogenic PAH concentrations at the on-site location are potential components of black carbon, a known byproduct of biomass burning, which can enhance soil carbon retention (Dutta et al., 2017; Wang et al., 2017). The role of black carbon in improving TOC and TN preservation has been demonstrated in many studies (Amoakwah et al., 2020; Ding et al., 2023; Dong et al., 2016; Huang et al., 2022; Joseph et al., 2020, and references therein). This link underscores how anthropogenic fire may have contributed to the nutrient dynamics in these soils. In contrast, the lower TOC and TN values observed at the near-site and off-site locations reflect edaphic conditions with minimal potential for human influence. These locales likely experienced different environmental conditions or supported different types of vegetation, leading to lower organic matter accumulation and more extensive decomposition (Rao et al., 2013; Song et al., 2014; Q. Wang et al., 2024; Wang et al., 2020).

The finding of this study is consistent with the hypothesis that the LK-IV was characterized by environmental conditions favorable to C_3 vegetation during human occupation. Many previous studies have highlighted the environmental influences of Pleistocene hunter-gatherers on landscape formation (Boivin et al., 2016; Braje and Erlandson, 2013; Hoag and Svenning, 2017; Malhi et al., 2016; Thompson et al., 2021a). One possible explanation for these depleted $\delta^{13}C$ values corresponds to the "Ecology of Fear" hypothesis, which posits that areas of repeated hominin habitation become dangerous for herbivores who perceive a predation threat, which drives them away (Thompson et al. 2021a). The reduced presence of large herbivores would have allowed natural vegetation succession to begin, wherein pioneer grass flora gave way to shrubs and was eventually overtaken by trees, leading to a more C_3-dominated landscape (Brown et al., 1999; Zanette and Clinchy, 2020, 2019). Another possibility is that human, controlled burning could have been used to manage the landscape, promoting the growth of favorable, fire-tolerant C_3 species by preventing the encroachment of C_4 grasses (Bowman and Haberle, 2010). The relatively heavier $\delta^{13}C$ values recorded at the OBM, KUL, and KH-II locales indicate more C_4 vegetation and the spread of grassy vegetation by non- or less-fear constrained herbivores or a lack of human-plant management activities.

The distribution of lithic artifacts across the study sites (fig. 1) provides crucial insights into the spatial patterns of human activity during MIS 15-11 (Anoikin et al., 2023; Ranov, 1995; Schäfer et al., 1998). The high concentration of lithic artifacts at on-site and sparse on-site locations aligns

with the isotopic evidence of depleted $\delta^{13}C$ values and elevated $\delta^{15}N$ values which could be result of repeated hominin occupation in this region in the past, which we interpret as having potentially impacted carbon and nitrogen cycling on the landscape, which has heretofore been documented in Holocene contexts (Ambrose and Sikes, 1991; Hedges and Reynard, 2007). Moreover, the few lithic artifacts found at PC 4 (Schäfer et al., 1998), a single artifact from PC 5, and none from PC 6 stratigraphic layers of KH-II (off-site) coupled with the soil isotopic data indicate that these areas were likely outside the regular scope of human activity. These off-site locations might have remained as natural landscapes with more C_4 or grassy C_3 vegetation and minimal human impact, which is reflected in the isotopic signatures that suggest lower organic input and a nitrogen cycle in tune with climate, rather than human-driven, selection pressures.

Several studies from Central, Western Europe, and China emphasize the importance of river shorelines, springs, and lakes in areas rich with dietary resources, freshwater, and lithic raw material during the Lower-Middle Palaeolithic (Antoine et al., 2016; Bae et al., 2018; Szymanek and Julien, 2018). Hominins in Central Europe adapted to a wide range of climates, with warmer, humid conditions favoring settlements, and they preferred forested or forest-steppe environments (Chu and Nett, 2021; Szymanek and Julien, 2018). Similarly, Sun et al. (2018) observed that hominin occupations in the Qinling Mountains of China were more frequent during interglacial periods, with a marked decline during glacial phases. Fox et al. (2023) similarly noted reduced human impact in less artifact-dense areas in the Eastern Qinling Mountains. Lu et al. (2011) found that Pleistocene hominins in the Luonan Basin, Central China, inhabited regions with a subtropical to warm-temperate climate, whereas Qin and Sun (2023) identified bidirectional hominin movements during glacial-interglacial cycles. Dennell et al. (2011) support the similarity of settlement patterns in Europe and China during the Middle Pleistocene. Our findings align with these global studies, showcasing how stable isotopes can illuminate human-environment interactions and highlight the universality of human resilience in adapting to climatic challenges during the Pleistocene, offering insights into human evolution and migration.

6. Conclusion

This study has provided insight into the complex interactions between early human interactions on Central Asian landscapes during MIS 15-11 through the analysis of isotopic signatures and soil organic matter content. The integration of $\delta^{13}C$ and $\delta^{15}N$ isotopic and TOC and TN data together

with lithic artifact distributions across different locations in the Khovaling region of Tajikistan has revealed patterns of early human activity and potential trends of anthropogenic influence on the terrain. At the on-site location, we observed elevated levels of $\delta^{15}N$, TOC, and TN values supplemented with high concentrations of lithic artifacts suggesting early hominin occupation, which could be likely due to the involvement of sustained subsistence practices and landscape management. Also, the same study location has recorded depleted $\delta^{13}C$ values indicating the occurrence of C_3/more closed-canopy vegetation consistent with enhanced winter-spring precipitation during interglacial periods. In contrast to this, near-site and off-site study locations exhibited lower $\delta^{15}N$, TOC, and TN values, and higher $\delta^{13}C$ values and lithic artifact densities indicating more open conditions and potentially less anthropogenically influenced in terms of their formation conditions. We caveat these findings with the understanding that post-depositional alterations of soil organic matter may have contributed to some of the observed variability, however, our results align with previous studies of spatial and temporal hetereogenity of land cover in the region (Chirakkal et al., 2025b, 2025a; Dodonov et al., 2006; Häggi et al., 2019; Shen et al., 2018; Wang et al., 2024; Yang and Ding, 2006; Zhao et al., 2022). These findings underscore the role of early human populations in shaping their environments with significant implications for understanding human adaptation and resilience in Central Asia during the Pleistocene.

CRediT authorship contribution statement

Aljasil Chirakkal: Conceptualization, Methodology, Validation, Formal analysis, Data curation, Investigation, Writing – original draft, Writing – review & editing, Visualization. **Ekaterina Kulakova:** Investigation, Data curation, Formal analysis, Writing – review & editing. **Jago Jonathan Birk:** Writing – review & editing, Supervision. **Anton Anoikin**: Writing – review & editing, Data curation, Investigation. **Redzhep Kurbanov**: Data curation, Investigation. **Piotr Sosin**: Data curation, Investigation. **Peixian Shu**: Data curation, Investigation. **David K. Wright:** Writing – review & editing, Conceptualization, Methodology, Formal analysis, Validation, Supervision, Project administration, Funding acquisition, Resources.

Acknowledgments

This research is supported by the Nordforsk (Project number: 105204) grant awarded to Dr. Jan-Pieter Buylaert (PI of the THOCA project, Technical University of Denmark, DTU). THOCA project participant Olga Meshcheryakova is grateful for the field preparation of the Khonako locale

for the study, and Olga Tokareva for the field preparation of the Obi-Mazar locale and conducting field magnetic susceptibility measurements of the Obi-Mazar and Lakhuti-IV locales. We want to thank Helen Wright who helped us to prepare isotope samples and William Hagopian (University of Oslo) and Pål Tore Mørkved (University of Bergen) for analyzing our samples in their laboratory.

References

Abramowski, U., Bergau, A., Seebach, D., Zech, R., Glaser, B., Sosin, P., Kubik, P.W., Zech, W., 2006. Pleistocene glaciations of Central Asia: results from 10Be surface exposure ages of erratic boulders from the Pamir (Tajikistan), and the Alay–Turkestan range (Kyrgyzstan). Quat. Sci. Rev. 25, 1080–1096. https://doi.org/10.1016/j.quascirev.2005.10.003

Ahmed, I.A.M., Maher, B.A., 2018. Identification and paleoclimatic significance of magnetite nanoparticles in soils. Proc. Natl. Acad. Sci. 115, 1736–1741. https://doi.org/10.1073/pnas.1719186115

Aizen, V.B., Aizen, E.M., Joswiak, D.R., Fujita, K., Takeuchi, N., Nikitin, S.A., 2006. Climatic and atmospheric circulation pattern variability from ice-core isotope/geochemistry records (Altai, Tien Shan and Tibet). Ann. Glaciol. 43, 49–60. https://doi.org/10.3189/172756406781812078

Ambrose, S.H., 1991. Effects of diet, climate and physiology on nitrogen isotope abundances in terrestrial foodwebs. J. Archaeol. Sci. 18, 293–317. https://doi.org/10.1016/0305-4403(91)90067-Y

Ambrose, S.H., Sikes, N.E., 1991. Soil Carbon Isotope Evidence for Holocene Habitat Change in the Kenya Rift Valley. Science 253, 1402–1405. https://doi.org/10.1126/science.253.5026.1402

Amoakwah, E., Arthur, E., Frimpong, K.A., Parikh, S.J., Islam, R., 2020. Soil organic carbon storage and quality are impacted by corn cob biochar application on a tropical sandy loam. J. Soils Sediments 20, 1960–1969. https://doi.org/10.1007/s11368-019-02547-5

Amundson, R., Austin, A.T., Schuur, E.A., Yoo, K., Matzek, V., Kendall, C., Uebersax, A., Brenner, D., Baisden, W.T., 2003. Global patterns of the isotopic composition of soil and plant nitrogen. Glob. Biogeochem. Cycles 17.

An, Z., Colman, S.M., Zhou, W., Li, Xiaoqiang, Brown, E.T., Jull, A.J.T., Cai, Y., Huang, Y., Lu, X., Chang, H., Song, Y., Sun, Y., Xu, H., Liu, W., Jin, Z., Liu, Xiaodong, Cheng, P., Liu, Y., Ai, L., Li, Xiangzhong, Liu, Xiuju, Yan, L., Shi, Z., Wang, X., Wu, F., Qiang, X., Dong, J., Lu, F., Xu, X., 2012. Interplay between the Westerlies and Asian monsoon recorded in Lake Qinghai sediments since 32 ka. Sci. Rep. 2, 619. https://doi.org/10.1038/srep00619

Anoikin, A., Sosin, P., Rybalko, A., Khudjageldiev, T., Sharipov, A., Karayev, A., Kulakova, E., Meshcheryakova, O., Tokareva, O., Kurbanov, R., 2023. Lakhuti-IV – A new site of the early Palaeolithic in Central Asia (Tajikistan). Archaeol. Res. Asia 35, 100466. https://doi.org/10.1016/j.ara.2023.100466

Antoine, P., coutard, S., Guerin, G., Deschodt, L., Goval, E., Locht, J.-L., Paris, C., 2016. Upper Pleistocene loess-palaeosol records from Northern France in the European context: Environmental background and dating of the Middle Palaeolithic. Quat. Int., Middle Palaeolithic in North-West Europe: Multidisciplinary Approaches 411, 4–24. https://doi.org/10.1016/j.quaint.2015.11.036

Aponte, C., Marañón, T., García, L.V., 2010. Microbial C, N and P in soils of Mediterranean oak forests: influence of season, canopy cover and soil depth. Biogeochemistry 101, 77–92. https://doi.org/10.1007/s10533-010-9418-5

Bae, C.J., Li, F., Cheng, L., Wang, W., Hong, H., 2018. Hominin distribution and density patterns in Pleistocene China: Climatic influences. Palaeogeogr. Palaeoclimatol. Palaeoecol., Cenozoic Climate Change in Eastern Asia - PART II 512, 118–131. https://doi.org/10.1016/j.palaeo.2018.03.015

Berger, A., Loutre, M.F., 1991. Insolation values for the climate of the last 10 million years. Quat. Sci. Rev. 10, 297–317. https://doi.org/10.1016/0277-3791(91)90033-Q

Bianchi, T.S., Mayer, L.M., Amaral, J.H.F., Arndt, S., Galy, V., Kemp, D.B., Kuehl, S.A., Murray, N.J., Regnier, P., 2024. Anthropogenic impacts on mud and organic carbon cycling. Nat. Geosci. 17, 287–297. https://doi.org/10.1038/s41561-024-01405-5

Boivin, N.L., Zeder, M.A., Fuller, D.Q., Crowther, A., Larson, G., Erlandson, J.M., Denham, T., Petraglia, M.D., 2016. Ecological consequences of human niche construction: Examining long-term anthropogenic shaping of global species distributions. Proc. Natl. Acad. Sci. 113, 6388–6396. https://doi.org/10.1073/pnas.1525200113

Bonafini, M., Pellegrini, M., Ditchfield, P., Pollard, A.M., 2013. Investigation of the 'canopy effect' in the isotope ecology of temperate woodlands. J. Archaeol. Sci. 40, 3926–3935. https://doi.org/10.1016/j.jas.2013.03.028

Boström, B., Comstedt, D., Ekblad, A., 2007. Isotope fractionation and 13C enrichment in soil profiles during the decomposition of soil organic matter. Oecologia 153, 89–98. https://doi.org/10.1007/s00442-007-0700-8

Boutton, T.W., 1991. Stable carbon isotope ratios of natural materials: 2 Atmospheric, terrestrial, marine, and freshwater environments. Academic Press, Inc, United States.

Bowman, D.M.J.S., Haberle, S.G., 2010. Paradise burnt: How colonizing humans transform landscapes with fire. Proc. Natl. Acad. Sci. 107, 21234–21235. https://doi.org/10.1073/pnas.1016393108

Braje, T.J., Erlandson, J.M., 2013. Human acceleration of animal and plant extinctions: A Late Pleistocene, Holocene, and Anthropocene continuum. Anthropocene, When Humans Dominated the Earth: Archeological Perspectives on the Anthropocene 4, 14–23. https://doi.org/10.1016/j.ancene.2013.08.003

Brown, J.S., Laundré, J.W., Gurung, M., 1999. The Ecology of Fear: Optimal Foraging, Game Theory, and Trophic Interactions. J. Mammal. 80, 385–399. https://doi.org/10.2307/1383287

Buchmann, N., Kao, W.-Y., Ehleringer, J., 1997. Influence of stand structure on carbon-13 of vegetation, soils, and canopy air within deciduous and evergreen forests in Utah, United States. Oecologia 110, 109–119. https://doi.org/10.1007/s004420050139

Buylaert, J.-P., Challier, A., Kulakova, E.P., Taratunina, N.A., Thomsen, K.J., Utkina, A.O., Sosin, P.M., Tokareva, O.A., Anoikin, A.A., Khujageldiev, T.U., A.C, K., Ubaydulloev, N.K., Murray, A.S., Kurbanov, R.N., 2024. A luminescence dating study of the upper part of the loess-palaeosol sequence at Kuldara, Khovaling Loess Plateau, Tajikistan. Quat. Geochronol. 101545. https://doi.org/10.1016/j.quageo.2024.101545

Caves, J.K., Winnick, M.J., Graham, S.A., Sjostrom, D.J., Mulch, A., Chamberlain, C.P., 2015. Role of the westerlies in Central Asia climate over the Cenozoic. Earth Planet. Sci. Lett. 428, 33–43. https://doi.org/10.1016/j.epsl.2015.07.023

Cerling, T.E., 1984. The stable isotopic composition of modern soil carbonate and its relationship to climate. Earth Planet. Sci. Lett. 71, 229–240. https://doi.org/10.1016/0012-821X(84)90089-X

Cerling, T.E., Quade, J., Wang, Y., Bowman, J.R., 1989. Carbon isotopes in soils and palaeosols as ecology and palaeoecology indicators. Nature 341, 138–139. https://doi.org/10.1038/341138a0

Cerling, T.E., Wynn, J.G., Andanje, S.A., Bird, M.I., Korir, D.K., Levin, N.E., Mace, W., Macharia, A.N., Quade, J., Remien, C.H., 2011. Woody cover and hominin environments in the past 6 million years. Nature 476, 51–56. https://doi.org/10.1038/nature10306

Challier, A., Thomsen, K.J., Kurbanov, R., Sosin, P., Murray, A., Guérin, G., Meshcheryakova, O., Karayev, A., Khormali, F., Taratunina, N., Utkina, A., Buylaert, J.-P., 2024. A detailed quartz and feldspar luminescence chronology for the Khonako II loess section (Southern Tajikistan). Quat. Geochronol. 83, 101571. https://doi.org/10.1016/j.quageo.2024.101571

Chang, K., 1987. The Archaeology of Ancient China. Yale University Press.

Chen, F., Chen, J., Huang, W., Chen, S., Huang, X., Jin, L., Jia, J., Zhang, X., An, C., Zhang, J., Zhao, Y., Yu, Z., Zhang, R., Liu, J., Zhou, A., Feng, S., 2019. Westerlies Asia and monsoonal Asia: Spatiotemporal differences in climate change and possible mechanisms on decadal to sub-orbital timescales. Earth-Sci. Rev. 192, 337–354. https://doi.org/10.1016/j.earscirev.2019.03.005

Cheng, H., Edwards, R.L., Sinha, A., Spötl, C., Yi, L., Chen, S., Kelly, M., Kathayat, G., Wang, X., Li, X., Kong, X., Wang, Y., Ning, Y., Zhang, H., 2016. The Asian monsoon over the past 640,000 years and ice age terminations. Nature 534, 640–646. https://doi.org/10.1038/nature18591

Cheng, H., Zhang, P.Z., Spötl, C., Edwards, R.L., Cai, Y.J., Zhang, D.Z., Sang, W.C., Tan, M., An, Z.S., 2012. The climatic cyclicity in semiarid-arid central Asia over the past 500,000 years. Geophys. Res. Lett. 39. https://doi.org/10.1029/2011GL050202

Chirakkal, A., Steindal, C.C., Birk, J.J., Kurbanov, R., Wright, D.K., 2025a. Occurrence and distribution of biomarkers in loess-paleosol sequences of Tajikistan (Central Asia): Implication for archaeo-ecological studies. J. Archaeol. Sci. Rep. 61, 104902. https://doi.org/10.1016/j.jasrep.2024.104902

Chirakkal, A., Stiendal, C.C., Birk, J.J., Újvári, G., Wright, D.K., 2025b. Biomarker evidence on early Paleolithic human-environment interactions from loess records in Tajikistan, Central Asia. Palaeogeogr. Palaeoclimatol. Palaeoecol. 112786. https://doi.org/10.1016/j.palaeo.2025.112786

Chu, W., Nett, J.J., 2021. The past in dust: current trends and future directions in Pleistocene geoarcheology of European loess. J. Quat. Sci. 36, 1279–1292. https://doi.org/10.1002/jqs.3388

Clemens, S.C., Yamamoto, M., Thirumalai, K., Giosan, L., Richey, J.N., Nilsson-Kerr, K., Rosenthal, Y., Anand, P., McGrath, S.M., 2021. Remote and local drivers of Pleistocene South Asian summer monsoon precipitation: A test for future predictions. Sci. Adv. 7, eabg3848. https://doi.org/10.1126/sciadv.abg3848

Commisso, R.G., Nelson, D.E., 2006. Modern plant δ15N values reflect ancient human activity. J. Archaeol. Sci. 33, 1167–1176. https://doi.org/10.1016/j.jas.2005.12.005

Crowley, B.E., Blanco, M.B., Arrigo-Nelson, S.J., Irwin, M.T., 2013. Stable isotopes document resource partitioning and effects of forest disturbance on sympatric cheirogaleid lemurs. Naturwissenschaften 100, 943–956. https://doi.org/10.1007/s00114-013-1094-6

Davis, R.S., Ranov, V.A., 1999. Recent work on the Paleolithic of Central Asia. Evol. Anthropol. Issues News Rev. 8, 186–193. https://doi.org/10.1002/(SICI)1520-6505(1999)8:5<186::AID-EVAN6>3.0.CO;2-R

DeNiro, M.J., 1987. Stable Isotopy and Archaeology. Am. Sci. 75, 182–191.

Dennell, R., 2013. Hominins, deserts, and the colonisation and settlement of continental Asia. Quat. Int., The Middle Palaeolithic in the Desert 300, 13–21. https://doi.org/10.1016/j.quaint.2012.12.002

Dennell, R., 2008. The Palaeolithic Settlement of Asia. Cambridge University Press.

Dennell, R.W., Martinón-Torres, M., Bermúdez de Castro, J.M., 2011. Hominin variability, climatic instability and population demography in Middle Pleistocene Europe. Quat. Sci. Rev., Early Human Evolution in the Western Palaearctic: Ecological Scenarios 30, 1511–1524. https://doi.org/10.1016/j.quascirev.2009.11.027

Ding, X., Li, G., Zhao, X., Lin, Q., Wang, X., 2023. Biochar application significantly increases soil organic carbon under conservation tillage: an 11-year field experiment. Biochar 5, 28. https://doi.org/10.1007/s42773-023-00226-w

Ding, Z.L., Ranov, V., Yang, S.L., Finaev, A., Han, J.M., Wang, G.A., 2002. The loess record in southern Tajikistan and correlation with Chinese loess. Earth Planet. Sci. Lett. 200, 387–400. https://doi.org/10.1016/S0012-821X(02)00637-4

Dodonov, A.E., 1991. Loess of Central Asia. GeoJournal 24, 185–194. https://doi.org/10.1007/BF00186015

Dodonov, A.E., 1986. Anthropogene of South Tajikistan. Mosc. Nauka 168.

Dodonov, A.E., Baiguzina, L.L., 1995. Loess stratigraphy of Central Asia: Palaeoclimatic and palaeoenvironmental aspects. Quat. Sci. Rev., Aeolian Sediments in the Quaternary Record 14, 707–720. https://doi.org/10.1016/0277-3791(95)00054-2

Dodonov, A.E., Gorshkov, A.I., Verkhovtseva, N.V., Sivtsov, A.V., Zhou, L.P., 2002. New Data on the Composition of Magnetic Minerals from Paleosols of Southern Tajikistan. Lithol. Miner. Resour. 37, 186–193. https://doi.org/10.1023/A:1014832718837

Dodonov, A.E., Sadchikova, T.A., Sedov, S.N., Simakova, A.N., Zhou, L.P., 2006. Multidisciplinary approach for paleoenvironmental reconstruction in loess-paleosol studies of the Darai Kalon section, Southern Tajikistan. Quat. Int., Loess and palaeoenvironments across Eurasia 152–153, 48–58. https://doi.org/10.1016/j.quaint.2005.12.001

Dodonov, A.E., Shackleton, N., Zhou, L.P., Lomov, S.P., Finaev, A.F., 1999. Geochronology, correlation, and evolution of paleoenvironments. Stratigr. Geol. Correl. 7, 66–80.

Dong, X., Guan, T., Li, G., Lin, Q., Zhao, X., 2016. Long-term effects of biochar amount on the content and composition of organic matter in soil aggregates under field conditions. J. Soils Sediments 16, 1481–1497. https://doi.org/10.1007/s11368-015-1338-5

Dutta, T., Kwon, E., Bhattacharya, S.S., Jeon, B.H., Deep, A., Uchimiya, M., Kim, K.-H., 2017. Polycyclic aromatic hydrocarbons and volatile organic compounds in biochar and biochar-amended soil: a review. GCB Bioenergy 9, 990–1004. https://doi.org/10.1111/gcbb.12363

Farquhar, G.D., Ehleringer, J.R., Hubick, K.T., 1989. Carbon Isotope Discrimination and Photosynthesis. Annu. Rev. Plant Biol. 40, 503–537. https://doi.org/10.1146/annurev.pp.40.060189.002443

Finestone, E.M., Breeze, P.S., Breitenbach, S.F.M., Drake, N., Bergmann, L., Maksudov, F., Muhammadiyev, A., Scott, P., Cai, Y., Khatsenovich, A.M., Rybin, E.P., Nehrke, G., Boivin, N., Petraglia, M., 2022. Paleolithic occupation of arid Central Asia in the Middle Pleistocene. PLOS ONE 17, e0273984. https://doi.org/10.1371/journal.pone.0273984

Forster, Th., Heller, F., 1994. Loess deposits from the Tajik depression (Central Asia): Magnetic properties and paleoclimate. Earth Planet. Sci. Lett. 128, 501–512. https://doi.org/10.1016/0012-821X(94)90166-X

Fox, M.L., Tierney, J., Lu, H., Wang, S., Xia, W., Zhang, H., Wu, J., 2023. Leaf wax isotopes reveal distinct hominin paleoenvironments in the Eastern Qinling Mountains of central China. Quat. Sci. Rev. 299, 107845. https://doi.org/10.1016/j.quascirev.2022.107845

Gao, X., Guan, Y., Xu, X., Olsen, J.W., 2017. Paleolithic Research in China, in: Habu, J., Lape, P.V., Olsen, J.W. (Eds.), Handbook of East and Southeast Asian Archaeology. Springer, New York, NY, pp. 241–276. https://doi.org/10.1007/978-1-4939-6521-2_18

Glantz, M.M., 2011. The History of Hominin Occupation of Central Asia in Review, in: Asian Paleoanthropology. Springer, Dordrecht, pp. 101–112. https://doi.org/10.1007/978-90-481-9094-2_8

Golubtsov, V.A., 2020. Stable Carbon Isotopic Composition of Organic Matter of the Late Pleistocene and Holocene Soils of the Baikal Region. Eurasian Soil Sci. 53, 724–738. https://doi.org/10.1134/S1064229320060046

Grogan, P., Burns, T.D., Chapin III, F.S., 2000. Fire effects on ecosystem nitrogen cycling in a Californian bishop pine forest. Oecologia 122, 537–544. https://doi.org/10.1007/s004420050977

Grove, M., 2014. Evolution and dispersal under climatic instability: a simple evolutionary algorithm. Adapt. Behav. 22, 235–254. https://doi.org/10.1177/1059712314533573

Guo, Z.T., Berger, A., Yin, Q.Z., Qin, L., 2009. Strong asymmetry of hemispheric climates during MIS-13 inferred from correlating China loess and Antarctica ice records. Clim. Past 5, 21–31. https://doi.org/10.5194/cp-5-21-2009

Habinger, S.G., Chavasseau, O., Jaeger, J.-J., Chaimanee, Y., Soe, A.N., Sein, C., Bocherens, H., 2022. Evolutionary ecology of Miocene hominoid primates in Southeast Asia. Sci. Rep. 12, 11841. https://doi.org/10.1038/s41598-022-15574-z

Häggi, C., Eglinton, T.I., Zech, W., Sosin, P., Zech, R., 2019. A 250 ka leaf-wax δD record from a loess section in Darai Kalon, Southern Tajikistan. Quat. Sci. Rev. 208, 118–128. https://doi.org/10.1016/j.quascirev.2019.01.019

Hao, Q., Wang, L., Oldfield, F., Guo, Z., 2015. Extra-long interglacial in Northern Hemisphere during MISs 15-13 arising from limited extent of Arctic ice sheets in glacial MIS 14. Sci. Rep. 5, 12103.

Hedges, R.E.M., Reynard, L.M., 2007. Nitrogen isotopes and the trophic level of humans in archaeology. J. Archaeol. Sci. 34, 1240–1251. https://doi.org/10.1016/j.jas.2006.10.015

Hoag, C., Svenning, J.-C., 2017. African Environmental Change from the Pleistocene to the Anthropocene. Annu. Rev. Environ. Resour. 42, 27–54. https://doi.org/10.1146/annurev-environ-102016-060653

Hofman-Kamińska, E., Bocherens, H., Borowik, T., Drucker, D.G., Kowalczyk, R., 2018. Stable isotope signatures of large herbivore foraging habitats across Europe. PLOS ONE 13, e0190723. https://doi.org/10.1371/journal.pone.0190723

Högberg, P., 1997. Tansley Review No. 95 15N natural abundance in soil-plant systems. New Phytol. 137, 179–203. https://doi.org/10.1046/j.1469-8137.1997.00808.x

Huang, R., Li, B., Chen, Y., Tao, Q., Xu, Q., Wen, D., Gao, X., Li, Q., Tang, X., Wang, C., 2022. Biochar Application Increases Labile Carbon and Inorganic Nitrogen Supply in a Continuous Monocropping Soil. Land 11, 473. https://doi.org/10.3390/land11040473

Huber, E., Bell, T.L., Adams, M.A., 2013. Combustion influences on natural abundance nitrogen isotope ratio in soil and plants following a wildfire in a sub-alpine ecosystem. Oecologia 173, 1063–1074. https://doi.org/10.1007/s00442-013-2665-0

Ibañez, M., Aljazairi, S., Leiva, M.J., Werner, R.A., Ghashghaie, J., Sebastià, M.T., 2021. Tree – Open Grassland Structure Drives Carbon And Nitrogen Cycling In Mediterranean Wood Pastures of The Iberian Peninsula. https://doi.org/10.21203/rs.3.rs-868173/v1

Jha, D.K., Patalano, R., Ilgner, J., Achyuthan, H., Alsharekh, A.M., Armitage, S., Blinkhorn, J., Boivin, N., Breeze, P.S., Devra, R., 2024. Preservation of plant-wax biomarkers in deserts: implications for Quaternary environment and human evolutionary studies. J. Quat. Sci.

Jia, J., Lu, H., Wang, Y., Xia, D., 2018. Variations in the Iron Mineralogy of a Loess Section in Tajikistan During the Mid-Pleistocene and Late Pleistocene: Implications for the Climatic Evolution in Central Asia. Geochem. Geophys. Geosystems 19, 1244–1258. https://doi.org/10.1002/2017GC007371

Jordanova, D., Petrovsky, E., Jordanova, N., Evlogiev, J., Butchvarova, V., 1997. Rock magnetic properties of recent soils from northeastern Bulgaria. Geophys. J. Int. 128, 474–488. https://doi.org/10.1111/j.1365-246X.1997.tb01569.x

Joseph, U.E., Toluwase, A.O., Kehinde, E.O., Omasan, E.E., Tolulope, A.Y., George, O.O., Zhao, C., Hongyan, W., 2020. Effect of biochar on soil structure and storage of soil organic carbon and nitrogen in the aggregate fractions of an Albic soil. Arch. Agron. Soil Sci. 66, 1–12. https://doi.org/10.1080/03650340.2019.1587412

Karimi Nezhad, M.T., Bruun, S., Magid, J., 2022. Depth profiles of soil organic carbon isotopes across a lithosequence: implications for drivers of soil δ13C vertical changes. Isotopes Environ. Health Stud. 58, 159–179. https://doi.org/10.1080/10256016.2022.2044806

Karkanas, P., 2010. Preservation of anthropogenic materials under different geochemical processes: A mineralogical approach. Quat. Int., Geoarchaeology and Taphonomy 214, 63–69. https://doi.org/10.1016/j.quaint.2009.10.017

Kingston, J.D., 2007. Shifting adaptive landscapes: Progress and challenges in reconstructing early hominid environments. Am. J. Phys. Anthropol. 134, 20–58. https://doi.org/10.1002/ajpa.20733

Kirsten, F., Dallmeyer, A., Bernbeck, R., Böhmer, T., Busch, R., Hessari, M., Pollock, S., Schütt, B., 2023. Were climatic forcings the main driver for mid-holocene changes in settlement dynamics on the Varamin Plain (Central Iranian Plateau)? PLOS ONE 18. https://doi.org/10.1371/journal.pone.0290181

Kramer, M.G., Sollins, P., Sletten, R.S., Swart, P.K., 2003. N Isotope Fractionation and Measures of Organic Matter Alteration During Decomposition. Ecology 84, 2021–2025. https://doi.org/10.1890/02-3097

Kulakova, E., Kurbanov, R., 2023. First Paleomagnetic Record of the Matuyama-Brunhes Transition in the Loess-Paleosol Series of Tajikistan, in: Kosterov, A., Lyskova, E., Mironova, I.,

Apatenkov, S., Baranov, S. (Eds.), Problems of Geocosmos—2022. Springer International Publishing, Cham, pp. 67–84. https://doi.org/10.1007/978-3-031-40728-4_6

Kutzbach, J.E., Chen, G., Cheng, H., Edwards, R.L., Liu, Z., 2014. Potential role of winter rainfall in explaining increased moisture in the Mediterranean and Middle East during periods of maximum orbitally-forced insolation seasonality. Clim. Dyn. 42, 1079–1095. https://doi.org/10.1007/s00382-013-1692-1

Larjavaara, M., Berninger, F., Palviainen, M., Prokushkin, A., Wallenius, T., 2017. Post-fire carbon and nitrogen accumulation and succession in Central Siberia. Sci. Rep. 7, 12776. https://doi.org/10.1038/s41598-017-13039-2

Lauer, F., Prost, K., Gerlach, R., Pätzold, S., Wolf, M., Urmersbach, S., Lehndorff, E., Eckmeier, E., Amelung, W., 2014. Organic Fertilization and Sufficient Nutrient Status in Prehistoric Agriculture? – Indications from Multi-Proxy Analyses of Archaeological Topsoil Relicts. PLOS ONE 9, e106244. https://doi.org/10.1371/journal.pone.0106244

Lazarenko, A.A., 1992. Loessic palaeolith. Content of conception and palaeoecological problems. Palaeoecol. Inhabitation Early Man North Asia Am. 141–147.

Li, Y., Song, Y., Kaskaoutis, D.G., Chen, X., Mamadjanov, Y., Tan, L., 2019. Atmospheric dust dynamics in southern Central Asia: Implications for buildup of Tajikistan loess sediments. Atmospheric Res. 229, 74–85. https://doi.org/10.1016/j.atmosres.2019.06.013

Liao, W., Hu, Jianfang, Zhou, H., Hu, Jianhua, Peng, P., Deng, W., 2018. Sources and distribution of sedimentary organic matter in the Beibu Gulf, China: Application of multiple proxies. Mar. Chem. 206, 74–83. https://doi.org/10.1016/j.marchem.2018.09.006

Lisiecki, L.E., Raymo, M.E., 2005. A Pliocene-Pleistocene stack of 57 globally distributed benthic δ18O records. Paleoceanography 20. https://doi.org/10.1029/2004PA001071

Lu, H., Zhang, H., Wang, S., Cosgrove, R., Sun, X., Zhao, J., Sun, D., Zhao, C., Shen, C., Wei, M., 2011. Multiphase timing of hominin occupations and the paleoenvironment in Luonan Basin, Central China. Quat. Res. 76, 142–147. https://doi.org/10.1016/j.yqres.2011.04.001

Lupien, R.L., Russell, J.M., Grove, M., Beck, C.C., Feibel, C.S., Cohen, A.S., 2020. Abrupt climate change and its influences on hominin evolution during the early Pleistocene in the Turkana Basin, Kenya. Quat. Sci. Rev. 245, 106531.

Machalett, B., Oches, E.A., Frechen, M., Zöller, L., Hambach, U., Mavlyanova, N.G., Marković, S.B., Endlicher, W., 2008. Aeolian dust dynamics in central Asia during the Pleistocene: Driven by the long-term migration, seasonality, and permanency of the Asiatic polar front. Geochem. Geophys. Geosystems 9. https://doi.org/10.1029/2007GC001938

Maher, B.A., 1998. Magnetic properties of modern soils and Quaternary loessic paleosols: paleoclimatic implications. Palaeogeogr. Palaeoclimatol. Palaeoecol. 137, 25–54. https://doi.org/10.1016/S0031-0182(97)00103-X

Malhi, Y., Doughty, C.E., Galetti, M., Smith, F.A., Svenning, J.-C., Terborgh, J.W., 2016. Megafauna and ecosystem function from the Pleistocene to the Anthropocene. Proc. Natl. Acad. Sci. 113, 838–846. https://doi.org/10.1073/pnas.1502540113

Mariotti, A., 1983. Atmospheric nitrogen is a reliable standard for natural 15N abundance measurements. Nature 303, 685–687. https://doi.org/10.1038/303685a0

Marshall, F., Reid, R.E.B., Goldstein, S., Storozum, M., Wreschnig, A., Hu, L., Kiura, P., Shahack-Gross, R., Ambrose, S.H., 2018. Ancient herders enriched and restructured African grasslands. Nature 561, 387–390. https://doi.org/10.1038/s41586-018-0456-9

Meshcheryakova, O.A., Kurbanov, R.N., Pavlov, V.E., 2023. Reconstructions of Paleowind Directions in the Pleistocene: Evidence from the Anisotropy of Magnetic Susceptibility of the Loess–Paleosol Series of Tajikistan and the Azov Region. Izv. Phys. Solid Earth 59, 704–716. https://doi.org/10.1134/S1069351323050063

Mestdagh, H., Haesaerts, P., Dodonov, A., Hus, J., 1999. Pedosedimentary and climatic reconstruction of the last interglacial and early glacial loess–paleosol sequence in South Tadzhikistan. CATENA 35, 197–218. https://doi.org/10.1016/S0341-8162(98)00100-3

Miao, Y., Herrmann, M., Wu, F., Yan, X., Yang, S., 2012. What controlled Mid–Late Miocene long-term aridification in Central Asia? — Global cooling or Tibetan Plateau uplift: A review. Earth-Sci. Rev. 112, 155–172. https://doi.org/10.1016/j.earscirev.2012.02.003

Natelhoffer, K.J., Fry, B., 1988. Controls on Natural Nitrogen-15 and Carbon-13 Abundances in Forest Soil Organic Matter. Soil Sci. Soc. Am. J. 52, 1633–1640. https://doi.org/10.2136/sssaj1988.03615995005200060024x

Novák, M., Buzek, F., Adamová, M., 1999. Vertical trends in δ13C, δ15N and δ34S ratios in bulk *Sphagnum* peat. Soil Biol. Biochem. 31, 1343–1346. https://doi.org/10.1016/S0038-0717(99)00040-1

O'Leary, M.H., 1988. Carbon isotopes in photosynthesis. Bioscience 38, 328–336.

Orland, I.J., He, F., Bar-Matthews, M., Chen, G., Ayalon, A., Kutzbach, J.E., 2019. Resolving seasonal rainfall changes in the Middle East during the last interglacial period. Proc. Natl. Acad. Sci. 116, 24985–24990. https://doi.org/10.1073/pnas.1903139116

Pakhomov, M.M., 2006. Glacial–Interglacial cycles in arid regions of northern Eurasia. Quat. Int., Loess and palaeoenvironments across Eurasia 152–153, 70–77. https://doi.org/10.1016/j.quaint.2006.02.018

Pardo, L.H., Hemond, H.F., Montoya, J.P., Fahey, T.J., Siccama, T.G., 2002. Response of the natural abundance of 15N in forest soils and foliage to high nitrate loss following clear-cutting. Can. J. For. Res. 32, 1126–1136. https://doi.org/10.1139/x02-041

Parviz, N., Shen, Z., Yunus, M., Zulqarnain, S., 2020. Loess deposits in southern Tajikistan (Central Asia): Magnetic properties and paleoclimate. Quat. Geochronol. 60, 101114. https://doi.org/10.1016/j.quageo.2020.101114

Patalano, R., Roberts, P., Boivin, N., Petraglia, M.D., Mercader, J., 2021. Plant wax biomarkers in human evolutionary studies. Evol. Anthropol. Issues News Rev. 30, 385–398. https://doi.org/10.1002/evan.21921

Penkov, A.V., Gamov, L.M., 1980. Paleomagnetic datums in the Pliocene to Quaternary strata of southern Tajikistan. In: The Neogene-Quaternary Boundary. Moscow: Nauka 184–189.

Potts, R., Faith, J.T., 2015. Alternating high and low climate variability: The context of natural selection and speciation in Plio-Pleistocene hominin evolution. J. Hum. Evol., Environmental Variability and Hominin Dispersal 87, 5–20. https://doi.org/10.1016/j.jhevol.2015.06.014

Qin, Z., Sun, X., 2023. Glacial–Interglacial Cycles and Early Human Evolution in China. Land 12, 1683. https://doi.org/10.3390/land12091683

Ranov, V., 2000. Loess-paleosol formation of Southern Tajikistan and Loess Palaeolithic. Arkheologicheskie raboty v Tadzhikistane. 21–49.

Ranov, V., 1995. The 'loessic palaeolithic' in South Tadjikistan, central Asia: Its industries, chronology and correlation. Quat. Sci. Rev., Aeolian Sediments in the Quaternary Record 14, 731–745. https://doi.org/10.1016/0277-3791(95)00055-0

Ranov, V., 1989. Does the terms 'Loessic Paleolithic'have a right for existence. Quat. Period Palaeontol. Archaeol. Kishinnew Shtiniza 137–145.

Ranov, V., Carbonell, E., Rodriguez, X.P., 1995. Kuldara: Earliest Human Occupation in Central Asia in Its Afro-Asian Context. Curr. Anthropol. 36, 337–346. https://doi.org/10.1086/204366

Ranov, V., Zhukov, V.A., 1979. Works of the group on the study of the Stone Age in 1974 Arkheologicheskie raboty v Tadzhikistane 14, 7–36.

Ranov, V.A., Davis, R.S., 1979. Toward a New Outline of the Soviet Central Asian Paleolithic.

Rao, Z., Xu, Y., Xia, D., Xie, L., Chen, F., 2013. Variation and paleoclimatic significance of organic carbon isotopes of Ili loess in arid Central Asia. Org. Geochem. 63, 56–63. https://doi.org/10.1016/j.orggeochem.2013.08.007

Rivas, Y., Huygens, D., Knicker, H., Godoy, R., Matus, F., Boeckx, P., 2012. Soil nitrogen dynamics three years after a severe Araucaria–Nothofagus forest fire. Austral Ecol. 37, 153–163. https://doi.org/10.1111/j.1442-9993.2011.02258.x

Roberts, P., Blumenthal, S.A., Dittus, W., Wedage, O., Lee-Thorp, J.A., 2017. Stable carbon, oxygen, and nitrogen, isotope analysis of plants from a South Asian tropical forest: Implications for primatology. Am. J. Primatol. 79, e22656. https://doi.org/10.1002/ajp.22656

Sage, R., Wedin, D.A., Li, M., 1999. C4 Plant Biology. Elsevier.

Sah, S.P., Rita, H., Ilvesniemi, H., 2006. 15N natural abundance of foliage and soil across boreal forests of Finland. Biogeochemistry 80, 277–288. https://doi.org/10.1007/s10533-006-9023-9

Schäfer, J., Ranov, V., Sosin, P.M., 1998. The "Cultural Evolution" of Man and the Chronostratigraphical Background of Changing Environments in the Loess Palaeosoil Sequences of Obi-Mazar and Khonako (Tadjikistan). Anthropologie 36, 121–135.

Shackleton, N.J., An, Z., Dodonov, A.E., Gavin, G., Kukla, G.J., Ranov, V.A., 1995. Accumulation rate of loess in Tajikistan and China : Relationship with global ice volume cycles. Quat. Proc. 4, 1–6.

Shahack-Gross, R., 2017. Archaeological formation theory and geoarchaeology: State-of-the-art in 2016. J. Archaeol. Sci. 79, 36–43. https://doi.org/10.1016/j.jas.2017.01.004

Shahgedanova, M., 2003. The Physical Geography of Northern Eurasia. Oxford University Press.

Shan, Y., Huang, M., Suo, L., Zhao, X., Wu, L., 2019. Composition and variation of soil δ15N stable isotope in natural ecosystems. CATENA 183, 104236. https://doi.org/10.1016/j.catena.2019.104236

Shen, J., Xiao, G., Wang, Z., Sun, Q., Wu, H., Zhang, C., Guo, Z., 2017. Distribution of n-alkanes in Miocene loess in Qinan, western Chinese Loess Plateau, and its palaeoenvironmental implications. Sci. China Earth Sci. 60, 921–928. https://doi.org/10.1007/s11430-016-9013-6

Shen, X., Wan, S., Colin, C., Tada, R., Shi, X., Pei, W., Tan, Y., Jiang, X., Li, A., 2018. Increased seasonality and aridity drove the C4 plant expansion in Central Asia since the Miocene–Pliocene boundary. Earth Planet. Sci. Lett. 502, 74–83. https://doi.org/10.1016/j.epsl.2018.08.056

Song, Y., Chen, X., Qian, L., Li, C., Li, Y., Li, X., Chang, H., An, Z., 2014. Distribution and composition of loess sediments in the Ili Basin, Central Asia. Quat. Int., ED@80: Loess in China and Europe - A Tribute to Edward Derbyshire 334–335, 61–73. https://doi.org/10.1016/j.quaint.2013.12.053

Still, C.J., Berry, J.A., Collatz, G.J., DeFries, R.S., 2003. Global distribution of C3 and C4 vegetation: Carbon cycle implications. Glob. Biogeochem. Cycles 17, 6-1-6–14. https://doi.org/10.1029/2001GB001807

Sun, X., Lu, H., Wang, S., Xu, X., Zeng, Q., Lu, X., Lu, C., Zhang, W., Zhang, X., Dennell, R., 2018. Hominin distribution in glacial-interglacial environmental changes in the Qinling Mountains range, central China. Quat. Sci. Rev. 198, 37–55. https://doi.org/10.1016/j.quascirev.2018.08.012

Szpak, P., 2014. Complexities of nitrogen isotope biogeochemistry in plant-soil systems: implications for the study of ancient agricultural and animal management practices. Front. Plant Sci. 5, 288. https://doi.org/10.3389/fpls.2014.00288

Szymanek, M., Julien, M.-A., 2018. Early and Middle Pleistocene climate-environment conditions in Central Europe and the hominin settlement record. Quat. Sci. Rev. 198, 56–75. https://doi.org/10.1016/j.quascirev.2018.08.021

Taft, J.B., Phillippe, L.R., Dietrich, C.H., Robertson, K.R., 2011. Grassland composition, structure, and diversity patterns along major environmental gradients in the Central Tien Shan. Plant Ecol. 212, 1349–1361. https://doi.org/10.1007/s11258-011-9911-5

Thompson, J.C., Wright, D.K., Ivory, S.J., 2021a. The emergence and intensification of early hunter-gatherer niche construction. Evol. Anthropol. Issues News Rev. 30, 17–27. https://doi.org/10.1002/evan.21877

Thompson, J.C., Wright, D.K., Ivory, S.J., Choi, J.-H., Nightingale, S., Mackay, A., Schilt, F., Otárola-Castillo, E., Mercader, J., Forman, S.L., Pietsch, T., Cohen, A.S., Arrowsmith, J.R., Welling, M., Davis, J., Schiery, B., Kaliba, P., Malijani, O., Blome, M.W., O'Driscoll, C.A., Mentzer, S.M., Miller, C., Heo, S., Choi, J., Tembo, J., Mapemba, F., Simengwa, D., Gomani-Chindebvu, E., 2021b. Early human impacts and ecosystem reorganization in southern-central Africa. Sci. Adv. 7. https://doi.org/10.1126/sciadv.abf9776

Toderich, K., Black, C.C., Juylova, E., Kozan, O., Matsuo, T.M.& N., 2007. C3/C4 plants in the vegetation of Central Asia, geographical distribution and environmental adaptation in relation to climate, in: Climate Change and Terrestrial Carbon Sequestration in Central Asia. CRC Press.

Tokareva, O.A., Lebedeva, M.P., Sosin, P.M., Ashurmadov, I.K., Khormali, F., Kurbanov, R.N., 2025. Structure and properties of paleosols of the last two interglacial cycles of the Khovaling Loess Plateau, Tajikistan (Obi–Mazar section). Quat. Res. 1–17. https://doi.org/10.1017/qua.2024.32

van der Merwe, N.J., Medina, E., 1991. The canopy effect, carbon isotope ratios and foodwebs in amazonia. J. Archaeol. Sci. 18, 249–259. https://doi.org/10.1016/0305-4403(91)90064-V

Wang, C., Wang, Y., Herath, H.M.S.K., 2017. Polycyclic aromatic hydrocarbons (PAHs) in biochar – Their formation, occurrence and analysis: A review. Org. Geochem. 114, 1–11. https://doi.org/10.1016/j.orggeochem.2017.09.001

Wang, G., Li, J., Ravi, S., Theiling, B., Burger, W., 2021. Fire changes the spatial pattern and dynamics of soil nitrogen (N) and δ15N at a grassland-shrubland ecotone. J. Arid Environ. 186, 104422. https://doi.org/10.1016/j.jaridenv.2020.104422

Wang, H., Li, H., Qiu, Y., Shu, P., Liu, Y., Liu, W., Sun, J., Du, S., Wang, J., Ambrose, S.H., 2024. Seasonal landscape variability advances Lantian hominin's recognition capacity to strategically adapt to changing environments. Quat. Sci. Rev. 336, 108786. https://doi.org/10.1016/j.quascirev.2024.108786

Wang, Q., Tang, X., Lei, J., Jia, J., Murodov, D., Wang, B., Yao, Z., Wang, X., Chen, J., 2024. Paleoclimatic significance of the organic carbon isotopes of the Tajikistan loess in arid Central Asia, on orbital timescales since the last interglacial. Palaeogeogr. Palaeoclimatol. Palaeoecol. 653, 112425. https://doi.org/10.1016/j.palaeo.2024.112425

Wang, Q., Wei, H., Khormali, F., Wang, L., Yan, H., Xie, H., Wang, X., Huang, W., Chen, J., Chen, F., 2020. Holocene Moisture Variations in Western Arid Central Asia Inferred From Loess Records From NE Iran. Geochem. Geophys. Geosystems 21, e2019GC008616. https://doi.org/10.1029/2019GC008616

Wynn, J.G., 2007. Carbon isotope fractionation during decomposition of organic matter in soils and paleosols: Implications for paleoecological interpretations of paleosols. Palaeogeogr. Palaeoclimatol. Palaeoecol. 251, 437–448. https://doi.org/10.1016/j.palaeo.2007.04.009

Wynn, J.G., Bird, M.I., Wong, V.N.L., 2005. Rayleigh distillation and the depth profile of 13C/12C ratios of soil organic carbon from soils of disparate texture in Iron Range National Park, Far North Queensland, Australia. Geochim. Cosmochim. Acta 69, 1961–1973. https://doi.org/10.1016/j.gca.2004.09.003

Yang, S., Ding, F., Ding, Z., 2006. Pleistocene chemical weathering history of Asian arid and semi-arid regions recorded in loess deposits of China and Tajikistan. Geochim. Cosmochim. Acta 70, 1695–1709. https://doi.org/10.1016/j.gca.2005.12.012

Yang, S., Ding, Z., 2006. Winter–spring precipitation as the principal control on predominance of C3 plants in Central Asia over the past 1.77 Myr: Evidence from δ13C of loess organic matter in Tajikistan. Palaeogeogr. Palaeoclimatol. Palaeoecol. 235, 330–339. https://doi.org/10.1016/j.palaeo.2005.11.007

Zanette, L.Y., Clinchy, M., 2020. Ecology and Neurobiology of Fear in Free-Living Wildlife. Annu. Rev. Ecol. Evol. Syst. 51, 297–318. https://doi.org/10.1146/annurev-ecolsys-011720-124613

Zanette, L.Y., Clinchy, M., 2019. Ecology of fear. Curr. Biol. 29, R309–R313. https://doi.org/10.1016/j.cub.2019.02.042

Zech, M., Zech, R., Glaser, B., 2007. A 240,000-year stable carbon and nitrogen isotope record from a loess-like palaeosol sequence in the Tumara Valley, Northeast Siberia. Chem. Geol. 242, 307–318. https://doi.org/10.1016/j.chemgeo.2007.04.002

Zeng, F., Xiang, S., Zhang, K., Lu, Y., 2011. Environmental evolution recorded by lipid biomarkers from the Tawan loess–paleosol sequences on the west Chinese Loess Plateau during the late Pleistocene. Environ. Earth Sci. 64, 1951–1963. https://doi.org/10.1007/s12665-011-1012-1

Zhao, J., An, C., Zhao, Y., Dong, W., 2022. Holocene C3/C4 vegetation variations in arid Central Asia: Implications for paleoclimate. Palaeogeogr. Palaeoclimatol. Palaeoecol. 592, 110905. https://doi.org/10.1016/j.palaeo.2022.110905

Zhou, W., Kong, X., Paterson, G.A., Sun, Y., Wu, Y., Ao, H., Xian, F., Du, Y., Tang, L., Zhou, J., Shi, Z., Jull, A.J.T., Zhao, G., An, Z., 2023. Eccentricity-paced geomagnetic field and monsoon rainfall variations over the last 870 kyr. Proc. Natl. Acad. Sci. 120, e2211495120. https://doi.org/10.1073/pnas.2211495120